NACA RM E54I16

NACA

RESEARCH MEMORANDUM

PENTABORANE COMBUSTION PERFORMANCE IN 9.75-INCH-DIAMETER RAM-JET ENGINE IN CONNECTED-PIPE ALTITUDE FACILITY

By Herschel J. Fivel, Leonard K. Tower, and James B. Gibbs

Lewis Flight Propulsion Laboratory
Cleveland, Ohio

NATIONAL ADVISORY COMMITTEE
FOR AERONAUTICS

WASHINGTON

March 13, 1957

Declassified October 28, 1960

NOTE

NACA Research Memorandum E54I16

By Herschel J. Fivel, Leonard K. Tower, and James B. Gibbs

At the time this report was written the best data available on the thermodynamic and physical properties of basic oxide were used in computing performance data. Investigations now in progress indicate that some of these properties may be inaccurate. For this reason absolute values of performance data presented herein must be viewed with caution. However, relative comparisons among different combustor configurations are probably valid.

NATIONAL ADVISORY COMMITTEE FOR AERONAUTICS

RESEARCH MEMORANDUM

PENTABORANE COMBUSTION PERFORMANCE IN 9.75-INCH-DIAMETER RAM-JET ENGINE IN CONNECTED-PIPE ALTITUDE FACILITY

By Herschel J. Fivel, Leonard K. Tower, and James B. Gibbs

3286

SUMMARY

The performance of pentaborane fuel was investigated in a flight-type, 9.75-inch-diameter ram-jet engine mounted in a connected-pipe altitude facility. A combustor configuration was developed that provided acceptable combustion performance for the equivalence-ratio range investigated, 0.10 to 0.93, and for combustor-inlet pressures of 3.6 to 29.9 pounds per square inch absolute. The configuration consisted of a fuel injector having three injection ports in each of eight tubes mounted radially on a central chamber, a 30-percent-blocked-area radial V-gutter flame holder with eight segments, and a combustion-chamber length of 45 inches.

Combustor efficiency was above 85 percent throughout the range of test conditions. At the richest equivalence ratio investigated, 0.93, the air-specific impulse value was 175 seconds. Satisfactory ignition and starting characteristics were displayed over an equivalence-ratio range of 0.10 to 0.52. All combustor parts withstood damage for the duration of the tests. Solid deposits, with a maximum layer thickness of 1/8 inch, were found on all combustor parts, but the engine performance was not affected. The data were extended to include the estimated performance of a flight vehicle along a proposed path of free-stream Mach number of 0.67 to 1.80.

INTRODUCTION

Specific fuels are being investigated at the NACA Lewis laboratory in an effort to extend the range, thrust, and operational limits of jet-propelled aircraft. Analytical impulse calculations indicate that boron hydride fuels, which have desirable heating values, are among those fuels that could provide range and thrust beyond that possible with hydrocarbon fuels (ref. 1). Aerodynamic analyses have predicted ranges from 30 to 50 percent greater than that of a hydrocarbon fuel for either diborane or pentaborane in a long-range, ram-jet powered aircraft; the value depends

upon the additional fuel-system weight assigned to handle the special fuel (refs. 2 and 3). The boiling points of diborane and pentaborane at sea-level pressure are -134° and 137° F, respectively. Therefore, pentaborane flight-type fuel-system weight penalties and handling problems should not be as severe as those expected for diborane.

Experimental investigations have indicated that the use of pentaborane may result in substantial gains in combustion stability because of the improvement it affords to flame speed and blow-out velocities. A small percentage of pentaborane in ethane increased the flame speed approximately 16-fold over that of ethane alone (ref. 4). The blow-out velocities (measured in a 2-in. diam. ram-jet combustor) of pentaborane-hydrocarbon fuel blends increased as the pentaborane concentration increased (ref. 5). Blow-out velocities of a 25-percent pentaborane-hydrocarbon blend were equal to the blow-out velocities of propylene oxide, a high-flame-speed fuel. Therefore, wide engine operational limits are anticipated for pure pentaborane.

3286

One of the problems anticipated in the use of fuels containing boron is the formation of solid boron oxide deposits on surfaces exposed to the combustion products. Although the boron oxide would exist as a liquid or vapor at combustor temperatures of interest, the oxide could exist near the combustor walls in the solid state, or the liquid oxide could be frozen as it made contact with the combustor wall. In short-duration tests in 2-inch-diameter combustors burning diborane (ref. 3) and pentaborane-hydrocarbon blends (ref. 5), boron oxide collected on the combustor walls, but the deposits were of insufficient quantity to interfere with normal operation of the combustor.

Flight tests using pentaborane fuel were planned for ram-jet vehicles of a previously investigated type in which gasoline was used (refs. 6 and 7). These vehicles were 16-inch-diameter, fin-stabilized, unguided units launched from a carrier plane at high altitudes. The vehicles were self-accelerated from subsonic to supersonic speeds. However, the engine diameter was reduced to 9.75 inches for this program with pentaborane in order to conserve fuel. The investigation reported herein was initiated to develop a fuel-injector and flame-holder configuration and fuel-handling techniques suitable for use in the 9.75-inch flight engine. Stable and efficient combustion, satisfactory ignition of the engine, adequate durability of combustor components, and freedom from excessive solid deposition were required for successful flight tests. A model which simulated the flight engine from the downstream portion of the diffuser to the combustor exit was mounted in a connected-pipe facility. The tests encompassed a range of combustor-inlet conditions nearly as wide as those predicted for the flight vehicle. The conditions investigated were as follows: inlet-air pressure, 3.55 to 29.9 pounds per square inch absolute; temperature 506° to 704° R; air flow, 1.62 to 16.26 pounds per second; equivalence ratio, 0.107 to 0.927. The performance is reported for several fuel-injector and flame-holder configurations

and two combustor lengths. Data for the best performing configuration are discussed in detail. In addition, the flight performance of the proposed engine is estimated from the combustion performance of the best configuration. The experimental program was conducted from October to December, 1953.

SYMBOLS

The following symbols are used in this report:

A	cross-sectional area, sq ft
B	barrel thrust, lb
C_F	thrust coefficient, $F/q_0A_{2,b}$
C_f	combustor force coefficient, $F/P_2A_{2,b}$
c	specific heat
F	total stream momentum at nozzle exit, lb
f/a	fuel-air ratio
g	acceleration due to gravity, 32.17 ft/sec^2
h	enthalpy, Btu/lb air
J	mechanical equivalent of heat, 778 ft-lb/Btu
M	Mach number
P	total pressure, lb/sq ft abs
p	static pressure, lb/sq ft abs
q	dynamic pressure, lb/sq ft
R	gas constant, (ft-lb)/(lb)($^\circ$R)
S_a	air specific impulse for M = 1, sec
S_f	fuel weight specific impulse for M = 1, sec
T	total temperature, $^\circ$R
t	static temperature, $^\circ$R

3286

V	velocity, ft/sec
v	specific volume, cu ft/lb gas
W	weight-flow rate, lb/sec
X	weight ratio of condensed products to total products
γ	ratio of specific heats
η	combustor efficiency
ρ	density, lb/cu ft
φ	equivalence ratio

Subscripts:

0	free stream
1	inlet plenum
2	diffuser exit
2,b	denotes effective combustor-inlet conditions, computed from density at station 2 and flow area equal to maximum combustor cross-sectional area
3	combustor exit
4	exit plenum
a	air
c	condensed
e	effective
f	fuel
g	gas
n	nozzle throat
p	constant pressure
T	based on total temperature
t	total
v	constant volume

3286

Superscript:

* conditions where M = 1

FUEL AND APPARATUS

Fuel. - The fuel used in this investigation was obtained through the cooperation of the Bureau of Aeronautics, Department of the Navy. Values of several of the physical properties of pure pentaborane are shown in the following table:

Formula weight	63.17
Melting point, °F	-52.3
Boiling point at 760 mm Hg, °F	137.1
Heat of combustion, Btu/lb	29,127
Heat of combustion, Btu/cu ft	1,166,741
Stoichiometric fuel-air ratio	0.0763
Density at 32° F, g/cc	0.643

Fuel-system and ram-jet installation. - A diagram of the fuel system is shown in figure 1. The fuel tank was fitted with a siphon extending to the bottom of the cylinder and a gas inlet located at the top of the cylinder. Fuel was forced from the tank by helium pressure, controlled by a remotely operated regulator. Fuel flow was started and stopped by a remotely controlled, pressure-operated piston valve. The fuel-flow rate was governed by the pressure-flow characteristics of the fuel injector and by the preset helium fuel-tank pressure.

The engine was mounted as shown in figure 2. Inlet and outlet ducts were connected to the laboratory air supply and the altitude exhaust system, respectively. The combustion air was metered, and then was throttled by a remotely controlled butterfly valve. The combustor wall was cooled by diverting a fixed portion of the incoming air (approximately 80 percent) through a 0.75-inch annulus between the wall and a cooling jacket before entering the engine. A window in the inlet plenum permitted visual observation of the flame.

The combustion products were discharged into a barrel-type thrust target mounted in the exhaust plenum. The gases, after being cooled by water sprays located in the barrel and the vertical duct, passed through a fixed-baffle separator and into either an exhaust stack and muffler or the throat of an air ejector and muffler for exhaust pressures below atmospheric.

Ram-jet engine. - The 9.75-inch-diameter connected-pipe engine used in the present investigation (fig. 2) simulates the internal dimensions of a scaled-down version of the 16-inch-diameter engines reported in references 6 and 7. The simulation begins at the aft section of the diffuser

3286

and continues to the combustor exit. The connected-pipe engine at the lower altitude test conditions had a straight pipe exit. However, in order to improve the accuracy of the thrust measurements at high-altitude conditions, a 7.25-inch-diameter convergent exhaust nozzle was used.

The fuel injector and the flame holder were attached to the aft end of the diffuser inner body, as shown in figure 3(a). The fuel injector had 24 ports of 0.0550-inch-diameter, all directed contrastream. Three ports were in each of eight tubes mounted radially on a central chamber. The ports were located so as to give as nearly a homogeneous fuel-air distribution in the inner 85 percent of the combustor area as possible. The fuel injector was located $3\frac{3}{4}$ inches upstream of the end of the flame holder. The flame holder was basically a V-gutter with 30-percent area blockage (fig. 3(b)). However, the "V" is extended $4\frac{1}{4}$ inches upstream of the fuel injector. This fuel injector and flame holder gave the best performance of any of the eight flame holders and five fuel injectors investigated during the development program, which is discussed in appendix A.

3286

Ignition was provided by a magnesium flare, 2 inches in diameter and $3\frac{1}{4}$ inches long, with a nominal burning time of 15 seconds. The flare was cemented into a tube which formed the center of the flame holder (fig. 3(b)). The downstream (ignition) face of the flare coincided with the trailing edge of the flame holder.

Instrumentation. - The combustion air flow was measured by a square-edged orifice conforming to A.S.M.E. standards. The fuel-flow rate was recorded continuously by means of a rotating-vane flowmeter (fig. 1) giving an electric signal to a self-balancing, recording potentiometer. A strain gage sensed the reaction of the thrust barrel to the exhaust jet force.

Inlet and exhaust plenum pressures, combustion-air orifice differential pressure, static and total pressures at station 2, and static pressures at station 3 (or n when an exhaust nozzle was used) were sensed by pressure transducers. These pressures and the strain-gage forces were indicated on an eight-channel oscillograph which recorded the data continuously as a function of time. The upstream orifice pressure was sensed by a pressure transducer and was indicated on a self-balancing potentiometer. In some of the tests, duplicate pressure measurements were obtained by using manometers.

Temperatures, recorded with self-balancing potentiometers, were measured with thermocouples at the following stations: combustion-air orifice, engine inlet, and combustor wall (six separate thermocouples at locations shown in fig. 2).

Temperatures at various stations in the fuel system were measured by thermocouples, but indicated on nonrecording potentiometers.

PROCEDURE

Choice of test conditions. - A proposed flight path was computed for the flight engine, using the data of reference 7 and assuming an exit temperature of 3000° R and a combustion efficiency of 90 percent. The engine would accelerate from the starting condition of $M_0 = 0.56$ at 35,000 feet altitude to $M_0 = 2.0$ at 13,500 feet altitude in 32.3 seconds, after which the fuel would be expended. Figure 4 shows the anticipated flight path. Combustor-inlet test conditions were chosen to simulate the flight conditions near the start of the flight, in the transonic region ($M_0 = 1.1$), and near the end of the flight. The flight conditions selected for simultation are indicated on figure 4 and the required combustor-operating conditions together with the actual test conditions are listed in the following table:

Anticipated flight conditions					Connected-pipe conditions			
Point	W_a, lb/sec	Equivalence ratio (η = 90%)	P_2, lb/sq in. abs	T_2, °R	W_a, lb/sec	Equivalence ratio	P_2, lb/sq in. abs	T_2, °R
1	1.8	0.45	4.6	430	2.1	0.23	4.9	517
2	5.4	.45	10.3	530	5.3	.46	10.2	537
3	15.0	.43	27.4	680	14.4	.43	26.8	643

Because of a limited air supply, the highest Mach number of the projected flight path that could be simulated was about 1.6. Unavailability of refrigerated air produced an inlet-temperature of about 90° F, which is too high for exact simulation of the initial part of the flight.

Calibration. - The thrust-measuring apparatus was calibrated with dead weights prior to and sometimes after each run. A check of the instrumentation was made before and after each run by obtaining steady-state, cold-flow data at several air flows and combustor pressures and comparing the recorded data with manometer and gage readings. In addition, the pressure-recording equipment was subjected to a comprehensive calibration approximately every five runs. The fuel flowmeter was calibrated with gasoline at intervals during the investigation and the measurements converted to pentaborane-flow rate by using a density-ratio correction factor.

Test procedure. - Combustion air was passed through the apparatus before each run to permit the inlet ducting to approach equilibrium temperature and to obtain cold-flow data. The air flow and the exit plenum

3286

pressure were preset at the desired test condition and the fuel lines were purged with helium. Pressure was applied to the fuel tank and the recorder chart drives were turned on. The flare was then ignited and the fuel valve was opened.

At low-altitude test conditions, where fuel-flow rates were high, the air flow was varied, in steps of decreasing flow, at about 5-second intervals, and then increased to the open-throttle starting condition. After a short time interval the fuel was shut off. For high-altitude test conditions, the fuel-flow rates were sufficiently low to permit a longer run without consumption of a large amount of fuel. Sufficient time was then allowed after ignition to permit the manometers to achieve equilibrium conditions. At each air flow, the manometer readings were recorded, either manually or photographically, after which the air flow was decreased and another steady-state point taken. The fuel-flow rate was then decreased, a final steady-state point taken, and the fuel shut off.

3286

Immediately after the fuel was shut off, helium was purged through the fuel injector and fuel-supply lines downstream of the fuel shut-off valve. After a 5-minute helium purge, the system was purged with gasoline and then again with helium. The engine was then disassembled and inspected for material failure and oxide deposition.

DATA REDUCTION

Data points were selected from the continuous records at conditions where the air- and fuel-flow rates, thrust, and combustor pressures were either constant or almost so. The combustor-inlet conditions were calculated assuming isentropic diffusion of air from the end of the diffuser to the maximum combustor area.

By determining the equivalence ratio φ_{ideal}, which should theoretically yield t_3, a combustor efficiency factor can be defined:

$$\eta = \left[\left(\frac{\varphi_{ideal}}{\varphi_{actual}}\right)_{(constant\ \ t_3)}\right]100 \qquad (1)$$

The combustor efficiency η compares the theoretical amount of fuel with the actual amount of fuel required to produce a given thrust level. It includes the effects of inefficient burning in the combustor, nozzle losses, heat losses to the combustor walls, and possible losses due to the flow characteristics of the heterogeneous exhaust products. The values of t_3 and M_3 are obtained from the relations

$$t_3 = \frac{p_3 A_3 V_3}{(1 - X) R_3 W_t} \tag{2}$$

$$M_3 = \frac{V_3}{\sqrt{(1 - X)\gamma_3 g R_3 t_3}} \tag{3}$$

3286

Equations (2) and (3) are presented in appendix B and their use is explained in appendix C.

The parameters used to evaluate the fuel performance were air and fuel specific impulses. They are a measure of the thrust-producing capability of the fuel-engine combination and account for the thermodynamic characteristics of the exhaust products. Air specific impulse is given by

$$S_a = F/W_a \ (F^*/F) \tag{4}$$

where F for the experimental data is derived in reference 8 and is expressed by

$$F = B + p_4 A_3 \tag{5}$$

Values of (F/F^*) for various values of γ_3 and M_3 are tabulated in reference 9. The fuel specific impulse is given by

$$S_f = F/W_f \ (F^*/F) = \frac{S_a}{f/a} \tag{6}$$

The combustor pressure losses were computed as the dimensionless ratio $P_2 - P_3/q_{2,b}$ and are customarily expressed as a function of the density ratio across the combustor:

$$\frac{\rho_{2,b}}{\rho_3} = \left(\frac{p_{2,b}}{R_2 t_2}\right)\left(\frac{R_3 t_3}{p_3}\right) \tag{7}$$

Another method of evaluating the thrust potential of a given combustor is by using the combustor force coefficient, derived and explained in reference 10. This coefficient

$$C_f = \frac{F}{P_2 A_{2,b}} \tag{8}$$

simplifies the accounting for the various pressure losses in the combustor. In addition, it is independent of all combustor environmental variables except inlet Mach number.

The predicted performance of the flight engine was calculated from the experimental values of the combustor force coefficient. With additional data from reference 7 for diffuser pressure losses, values for the thrust coefficient and the corresponding specific fuel consumption were determined. The thrust coefficient was calculated as follows:

$$C_T = \frac{W_a\left(\frac{F}{W_a} - \frac{V_0}{g}\right) - p_0 A_3}{q_0 A_{2,b}} \qquad (9)$$

3286

PRECISION OF DATA

The primary parameter, combustor efficiency, used to express combustor performance was determined from thrust measurements. The air specific impulse values were also computed after determining the exhaust-gas stream total momentum. Reference 8 points out that the thrust barrel provides an accurate method of determining thrust, particularly at low values of nozzle expansion ratio. Thus, the error in B depends on the accuracy of the instrumentation. The high-response-rate recording instruments had an error of ±2 percent at full-scale reading.

For tests at simulated low-altitude conditions, the exit plenum pressure p_4 was obtained from atmospheric pressure and the difference between atmospheric pressure and p_4. Since the difference value was in error by only 2 percent, the value of p_4 had only 1/2 percent error. Although steady-state calibration checks were made at high-altitude conditions, the error remained an estimated 1/2 percent. The expected error in the total stream momentum $B + p_4 A_3$ was of the order of 2.5 percent.

By careful choice of instrument ranges, the probable error in the air-flow measurement was maintained at about 1 percent for all test conditions. The fuel-flow error was maintained to within 2 percent. Thus, the air specific impulse was estimated to be in error by 3.5 percent.

The combustor-outlet velocity depended on the thrust measurement and the total mass flow through the engine. Errors in this velocity were estimated at 3 percent. Errors in the outlet temperature (which is obtained from the velocity) were estimated at around 5 percent. An examination of the slopes of the temperature - equivalence-ratio curves for pentaborane presented in reference 11 shows the magnifying effect errors in the outlet temperature have on the ideal equivalence ratio and, subsequently, on the combustor efficiency. The error in ideal equivalence ratio was estimated at 17 percent for temperatures in the region around 3000° R where the liquid exhaust products vaporize. This

corresponds to a 20 percent error in the combustor efficiency. Operation in the region of outlet temperatures of approximately 5000° R also produced the same magnitude of error. The error in ideal equivalence ratio for the remaining temperature regions was only about 9 percent with a corresponding error of 12 percent in the combustor efficiency.

RESULTS AND DISCUSSION

Connected-Pipe Performance

The engine development program (appendix A) included an investigation of the effect of five fuel-injector configurations, eight flame holders, and two combustor lengths. Resulting from this program was a combustor configuration which exhibited the best over-all performance of the configurations investigated. It contained the following components: fuel injector C (fig. 17(c)), 24 fixed-area orifices directed contrastream; flame holder H (fig. 18(h)), an elongated V-gutter-type blocking 30 percent of the combustor area; combustor of 45 inches length; ignition device, a 2-inch-diameter, $3\frac{1}{8}$-inch-long, centrally mounted magnesium flare. The advantages of such a design are as follows: Because of the high reactivity of the fuel, burning upstream of the rear face of the flame holder was anticipated to cause burnout of a simple V-gutter flame holder. By maintaining passages of constant area between the fuel-injector station and the downstream end of the flame holder, a high velocity is produced at the fuel-injector station. This reduces the tendency for burning upstream of the end of the flame holder and improves the atomization of the fuel. In addition, the elongated "V" design produces a sheltered zone of constant area even though it is progressively burned away from its downstream end. Table I presents the primary data and the following paragraphs discuss the performance obtained with this combustor configuration. For high-altitude conditions (start of flight test) a 7.25-inch-diameter convergent exhaust nozzle was added to improve the accuracy of the thrust determination. At low-altitude conditions, some data were obtained without a flame holder.

Combustor efficiency. - Combustor efficiency of the best-performing configuration is shown in figure 5 as a variation of equivalence ratio. Points obtained in less than 2.0 seconds from the start of each run were ignored when fairing the curves and are presented only to show that the engine was up to operating conditions in a short length of time.

The combustor efficiency was above 85 percent throughout the range of test conditions, which included equivalence ratios from 0.107 to 0.927. These data were cross-plotted at an equivalence ratio of 0.45, the proposed flight condition, and are presented in figure 6 as a function of combustor-inlet pressure. The combustor efficiency increased from 89 to 96 percent as the inlet pressure increased from 5.7 to 28.3

3286

pounds per square inch absolute. Combustor-inlet temperature and velocity varied, in addition to the combustor pressure, and the effects of these variables are included in the data of figure 6.

Air specific impulse. - Air specific impulse is presented as a variation of equivalence ratio in figure 7. Included in figure 7 are ideal pentaborane performance curves for the combustor operating conditions encountered in the experimental work. The air specific impulse increased with increasing equivalence ratio. It remained near ideal values throughout the range of equivalence ratios despite the wide range of inlet conditions. Impulse values of 90 and 175 seconds were achieved with pentaborane at equivalence ratios of 0.10 and 0.93, respectively.

3286

Fuel specific impulse. - The variation of the reciprocal of fuel specific impulse (specific fuel consumption) with air specific impulse is shown on figure 8. Again, ideal curves for pentaborane are presented. The actual fuel consumption does not exceed the theoretical by more than 15 percent at any of the conditions investigated.

Combustor-inlet conditions. - Combustor-inlet conditions of pressure, velocity, and Mach number are presented in figure 9. The inlet temperature remained constant for each run. Curves of constant fuel flow are drawn through the data points. The combustor-inlet conditions ranged as follows: pressure, 3.5 to 30.0 pounds per square inch absolute; velocity, 142 to 265 feet per second; Mach number, 0.128 to 0.211; and temperature, 46° to 200° F.

Combustor pressure losses. - The combustor total-pressure loss between stations 2 and 3 is shown in figure 10. The solid line drawn on the figure represents the sum of the theoretical momentum pressure losses due to heat addition, and the isothermal pressure losses as determined by cold-test data. This curve of predicted pressure loss is followed closely by the measured pressure losses. The considerably smaller pressure losses of runs 8 and 9 are to be expected, since runs 8 and 9 were made without a flame holder.

Combustor force coefficient. - Shown in figure 11 is the variation of combustor force coefficient with combustor-inlet Mach number. Theoretical curves of combustor force coefficient both with a 7.25-inch-diameter exit nozzle and without an exit nozzle are presented for combustor frictional total-pressure losses of 0, 2, and 4q. Experimental pressure losses, excluding those due to heat addition, are seen to vary from 0 to 3q under operating conditions both with and without an exit nozzle. Experimental data for the 7.25-inch-diameter exit nozzle were obtained at an exit Mach number of 1.0. The value of the combustor force coefficient to be used in the predicted flight-performance computations may be considered constant at 0.972 for the range of conditions of interest, since the proposed flight vehicle has no exit nozzle.

Solid deposition. - After each run solid deposits were found on all internal surfaces of the combustion chamber including parts of the fuel injector and the flame holder. Typical deposits on the fuel injectors and the flame holder are shown in figure 3, while the deposits on the combustor walls are typified by those shown in figure 12. In general, the total deposits increased as the total fuel used per run increased and as the simulated altitude increased. Maximum deposit thickness on the combustor wall was about 1/8 inch. An analysis of deposition effects based on deposits found after each run was complicated by several factors: (1) Equilibrium was probably not obtained in the short-duration runs; and (2) the appearance of deposits during combustion probably was quite different from deposits existing after the run, since residual fuel in the line continued to burn after the purge cycle was started. The deposits did not measurably affect the engine performance, since the combustor pressure losses did not increase with time during the runs (table I).

3286

Ignition. - The single magnesium flare provided satisfactory ignition for the entire range of conditions investigated: equivalence ratio, 0.10 to 0.52; combustor-inlet static pressure, 4 to 30 pounds per square inch absolute; and inlet static temperature, 46° to 217° F. The combustor-inlet velocities associated with the starting conditions were higher than the normal inlet velocities listed in table I. Shift of flare position from the center to the wall or to near the exit had no effect. Direction of the flare also produced no noticeable effect on ignition.

Attempts made to ignite without a flare resulted in autoignition at the simulated low-altitude condition. Autoignition did not occur at simulated high-altitude conditions.

Engine durability. - No engine damage was visible in the five short tests presented. In general, the cooling system was adequate for the short-durations tests that were employed, although the external combustor-wall temperature, measured $1\frac{3}{4}$ inches upstream of the exit, was still increasing at the end of a run (table I).

Combustion stability. - At all the conditions investigated, combustion was smooth and stable. Stable combustion also occurred throughout the combustor development program described in appendix A for several of the combustor configurations. The exceptional qualities of the fuel were further demonstrated by the continued burning of fuel being purged from the lines into the burner. The flame was observed to gradually dim, and at no time did a sharp flame-out occur; thus burning was sustained at extremely low fuel-air ratios.

Estimated Flight Performance

Thrust coefficients and specific fuel consumptions were computed for the flight vehicle by using experimental data presented herein to determine thrust values and data from reference 7 for diffuser pressure losses.

Simulated flight conditions. - The ranges of the combustor-inlet parameters encountered during the investigation corresponded to three widely separated flight test conditions. As indicated in figure 4, these conditions simulated flight free-stream Mach numbers of 0.67, 1.10, and 1.63, corresponding to altitudes of 33,000, 26,000, and 17,500 feet, respectively. Also chosen for analysis was the condition at the diffuser design Mach number of 1.80 for an altitude of 15,500 feet. Since the necessary experimental data at a Mach number of 1.8 were unavailable, experimental data for a condition simulating Mach 1.63 were used. For each condition, then, values of thrust coefficient and specific fuel consumption were determined for an operating equivalence-ratio range of 0.2 to 0.5.

3286

Thrust coefficient. - Figure 13 presents the variation of the thrust coefficient with equivalence ratio for four flight Mach numbers. For the equivalence-ratio range of 0.2 to 0.5, the coefficients increase with increasing fuel flow. Inflections of the two lower curves are due to the vaporization of liquid oxide in the exhaust stream in the temperature region involved. A cross plot of figure 13 at the proposed operating equivalence ratio of 0.45 is presented in figure 14. For the flight operating condition, the thrust coefficient increases as the flight Mach number increases. Near the end of the flight, at the design Mach number of 1.8, the thrust coefficient starts to level off sharply at a value of 0.8.

Thrust specific fuel consumption. - Thrust specific fuel consumption is presented in figure 15. Fuel consumption rises with increased equivalence-ratio operation. It also appears to rise when the equivalence ratio is sufficiently lowered. Figure 16 presents the fuel consumption along the flight path for the proposed operating equivalence ratio of 0.45. The fuel consumption drops off sharply at the beginning of the flight and levels off at a fuel consumption value of 2.1 pounds of fuel per hour per pound thrust towards the end of the flight.

SUMMARY OF RESULTS

An investigation of a 9.75-inch-diameter connected-pipe ram-jet engine using pentaborane fuel was conducted to develop a combustor configuration and fuel-handling techniques suitable for use in a flight engine. The results are as follows:

1. A combustor was developed for pentaborane fuel that provided acceptable combustion performance for equivalence ratios between 0.107 and 0.927 for combustor-inlet pressures between 3.6 and 29.9 pounds per square inch absolute, and for combustor-inlet temperatures between 46° and 200° F. Combustion limits were not determined.

2. Combustor efficiencies of 89 and 96 percent were obtained at combustor-inlet pressures of 5.7 and 28.3 pounds per square inch absolute for an equivalence ratio of 0.45.

3286

3. An air specific impulse of 175 seconds was obtained at an equivalence ratio of 0.93.

4. When evaluated under burning conditions, the combustor frictional pressure losses ranged from 0 to 3q (where q is dynamic pressure).

5. Ignition of the ram-jet engine was successfully accomplished by an electrically fired magnesium flare at pressures of 4 to 30 pounds per square inch absolute over an equivalence-ratio range of 0.10 to 0.52.

6. The deposition of solid combustion products was confined to a thin layer on the combustor walls and on the fuel injector and flame holder. This deposition did not affect the combustion performance for the small amounts of fuel used in each test. The durability of all combustor parts was satisfactory.

7. The flight performance of a 9.75-inch-diameter ram-jet engine was estimated from the combustion performance reported herein and diffuser recovery data obtained from ram-jet engine data reported previously.

Lewis Flight Propulsion Laboratory
National Advisory Committee for Aeronautics
Cleveland, Ohio, September 15, 1954

APPENDIX A

CONFIGURATION DEVELOPMENT

The program presented herein was directed towards the development of a combustor for use in a particular flight vehicle. The flight vehicle was a scaled-down model of a type of ram-jet engine investigated in references 6 and 7. Reduction of the engine diameter to 9.75 inches was necessary in order to conserve fuel, which was available in limited quantities. The total amount of fuel used in the program, configuration development and evaluation of final design, was 92.8 pounds. Eight flame holders, five fuel injectors, and two combustor lengths were investigated (figs. 17 and 18). The combustor efficiencies achieved by the various combustor configurations is presented against equivalence ratio in figure 19.

3286

Location of the fuel system in the diffuser center body of the flight vehicle suggested the use of a single-point injector mounted on the aft end of the diffuser. This injector was a pintle-type nozzle with the pintle grooved to produce eight streams of fuel. This injector with a 50° shroud (fig. 17(a)) was tested with flame holders A, B, and C (fig. 18)). Only flame holder B (represented in fig. 19 by run 3) gave results high enough to be plotted.

These poor results indicated that a homogeneous fuel-air distribution was perhaps more desirable than locally fuel-rich zones. Data in reference 12 suggested the use of multiple orifices, injecting contrastream to the air flow. Fuel injector B, 12 orifices, was used with flame holder A in run 4, the results of which are shown in figure 19.

Flame holders D and E were attempts to further atomize the fuel spray by providing a high-velocity region around injector B, still retaining the V-gutter flame-holding qualities. These designs improved the efficiency slightly, as indicated by runs 5 and 6 (fig. 19). Better spray characteristics and distribution were obtained with injector C: 8 spokes, 24 orifices, contrastream. Results without a flame holder are indicated by run 7.

Increasing the combustor length from 27 inches to 45 inches greatly improved the efficiency over run 7, as indicated by runs 8 and 9. Although the efficiencies of runs 8 and 9 indicated a flame holder was not needed, use of flame holder H was necessary to insure smooth operation at the starting conditions of the flight test (400° R and 3.72 lb/sq in. abs.). The efficiency did not noticeably change with the addition of the flame holder. This flame holder and fuel injector C provided the final design, to be evaluated further and used in the flight vehicle.

Other configurations were injector D used with splash plates and located upstream of flame holder F, and fuel injector E with flame holder G. These results are represented by runs 10 and 11, respectively.

APPENDIX B

THERMODYNAMICS OF FLOWING GAS STREAMS CONTAINING FINELY DIVIDED PARTICLES IN VELOCITY AND TEMPERATURE EQUILIBRIUM

3286

In this report it has been assumed that any particles of condensed boric oxide are sufficiently small to be in both velocity and temperature equilibrium with the flowing gas. The assumption has also been made that the volume of solids is negligible. The conventional equations for compressible flow can be written for gas streams containing finely divided particles provided (1) allowance is made for the weight ratio X of condensed products to total products, and (2) the value of $\bar{\gamma}$ is defined as

$$\bar{\gamma} = \frac{\bar{c}_p}{\bar{c}_v} \tag{B1}$$

where

$$c_p = Xc_c + (1 - X)\, c_p \tag{B2}$$

and

$$\bar{c}_v = Xc_c + (1 - X)\left(c_p - \frac{R}{J}\right) \tag{B3}$$

Flow equations for the two-phase system then may be expressed as follows:

Isentropic pressure-temperature relations:

$$\frac{p}{p_1} = \left(\frac{t}{t_1}\right)^{\frac{\bar{\gamma}}{\bar{\gamma}-1}} \tag{B4}$$

and

$$\frac{p}{p_1} = \left(\frac{\rho_g}{\rho_{g,1}}\right)^{\bar{\gamma}} \tag{B5}$$

Speed of sound:

$$V^* = \sqrt{(1 - X)\,\bar{\gamma} g R t} \tag{B6}$$

Mach number:

$$M = \frac{V}{\sqrt{(1 - X)\,\bar{\gamma} g R t}} \tag{B7}$$

Ratio of total to static temperature:

$$\frac{T}{t} = 1 + \frac{\bar{\gamma} - 1}{2} M^2 \tag{B8}$$

Velocity resulting from isentropic expansion of mixture:

$$V = \sqrt{2gR\,(1 - X)\,\frac{\bar{\gamma}}{\bar{\gamma} - 1}\,T_1 \left[1 - \left(\frac{p_2}{p_1}\right)^{\frac{\bar{\gamma}-1}{\bar{\gamma}}}\right]} \tag{B9}$$

Equation of continuity:

$$W_t = \frac{pAV}{(1 - X)Rt}$$

or

$$W_t = \frac{PAM\sqrt{\frac{\bar{\gamma} g}{(1 - X)RT}}}{\left(1 + \frac{\bar{\gamma} - 1}{2} M^2\right)^{\frac{\gamma+1}{2(\gamma-1)}}} \tag{B10}$$

Momentum equation:

$$F = pA\,(1 + \bar{\gamma} M^2)$$

or

$$F = \frac{W_t}{M}\sqrt{\frac{(1 - X)RT}{\bar{\gamma} g\left(1 + \frac{\bar{\gamma} - 1}{2} M^2\right)}}\,(1 + \bar{\gamma} M^2) \tag{B11}$$

3286

3286

APPENDIX C

CHARTS FOR DETERMINING STATIC COMBUSTION TEMPERATURE AND THERMAL PROPERTIES OF COMBUSTION PRODUCTS OF PENTABORANE

Combustor-outlet static temperature. - Reference 11 presents curves of combustion temperature, for which negligible velocities at both the combustor inlet and outlet are assumed. In actual practice, the high combustor-outlet velocity causes the kinetic energy to be an appreciable fraction of the total energy possessed by the gases. The static combustor-outlet temperatures will then be less than those indicated by the curves of reference 11. This reduction in combustor-outlet static temperature may be accompanied in some cases by shifts in chemical and physical equilibria. The static temperatures with appreciable velocity then cannot be related to the temperature data of reference 11 for zero combustor-outlet velocity by the conventional relation:

$$t_M = \frac{t_{(M=0)}}{1 + \frac{\gamma - 1}{2} M^2}$$

In particular, this expression is unsuitable when a boron-containing fuel is burned at temperatures such that both liquid and gaseous boric oxide are formed simultaneously. It is therefore necessary to allow for the kinetic energy of the combustor products when the static combustion temperature is determined for boron-containing fuels.

A series of curves has been devised for the combustion products of pentaborane-air mixtures by means of which the static combustion temperature can be determined for an appreciable combustor-outlet velocity. Allowance is made for the kinetic energy of the exhaust gases by subtracting this energy from the combustor-inlet air enthalpy, thus yielding an effective combustor-inlet air enthalpy

$$h_{a,e} = h_{a,T,2} - \frac{V_3^2}{2gJ} \qquad (C1)$$

Figure 20 may be used to determine the value of the actual inlet-air total enthalpy from the inlet-air total temperature.

The variation of combustor-outlet static temperature with combustor static pressure for effective inlet-air enthalpies of 110, 245, and 445 Btu per pound air is presented in figures 21(a), (b), and (c), respectively. For intermediate inlet-air enthalpies, the data of figures 21(a), (b), and (c) may be cross-plotted on an interpolation chart (fig. 21(d)). Some examples will illustrate the cross-plotting techniques and use of the curves.

Assume that the variation of outlet temperature with effective inlet-air enthalpy is desired for a range of equivalence ratios at an outlet static pressure of 2 atmospheres. This family of curves is constructed on the interpolation chart (fig. 21(d)). To aid the construction of these curves, included on the chart is a family of curves representing the variation of the saturation temperature with effective inlet-air enthalpy at various combustion pressures.

At an equivalence ratio of 0.3 and a combustion pressure of 2 atmospheres, combustion temperatures of 2380°, 2785°, and 3160° R are read from figures 21(a), (b), and (c), respectively. These temperatures are plotted on the interpolation chart and are connected by the curve ABC. All three points lie in the two-phase region, since the curve on figure 21(d) does not cross the 2-atmospheres pressure line.

3286

When sufficiently high equivalence ratios are reached, the temperature on one or more of the pressure-temperature charts may lie in the gaseous region, or above the saturation line. At an equivalence ratio of 0.48 and 2 atmospheres pressure, temperatures of 3190°, 3370°, and 3920° R are read from figures 21(a), (b), and (c), respectively. The latter two points lie in the gaseous region and can be connected with reasonable accuracy by a straight line DE. Extending line DE to the 2-atmospheres pressure curve determines the point G at which liquid starts to condense. The variation of temperature with enthalpy in the two-phase region is not linear. Since only two points are available to determine the remainder of the 0.48 equivalence-ratio curve, a curve FG must be approximated by the straight line FG.

Only one point, K, at an equivalence ratio of 0.40 lies in the gaseous region. Point J is located by drawing a line through K parallel to an equivalence ratio line having two points in the gaseous region, such as DE, and extending to the proper combustion pressure curve. A smooth curve HIJ may be drawn in the two-phase region to complete the line HIJK.

Thermal properties of combustion products. - Three thermal properties, ratio of specific heats γ, gas constant R, and weight ratio of condensed products to total products X are presented in figure 22, which is similar to figure 21 for combustion temperature. Values of these properties as a function of effective inlet-air enthalpy at various pressures and equivalence ratios are obtained by the use of the accompanying interpolation chart. Examples at the same conditions as in the previous discussion will illustrate the use of these charts.

Consider an equivalence ratio of 0.30 at a pressure of 2 atmospheres. Values of 54.93, 54.87, and 53.38 foot-pounds per pound °R for the gas constant from figures 22(a), (b), and (c), respectively, are plotted as points A, B, and C on the interpolation curve (fig. 22(d)). A smooth curve ABC may be drawn through the three points since all lie in one region. At an equivalence ratio of 0.48, the point of transition

from two phases to a single phase must be determined. Values of R from figures 22(b) and (c), plotted as points D and E on the interpolation chart, lie in the gaseous region and may be connected by a straight line DE. Extending line DE to the 2-atmospheres pressure curve determines the transition point G for a combustion pressure of 2 atmospheres. The remaining point, F, in the two-phase region, may be connected to G by a straight line, although FG should properly be a curved line. At an equivalence ratio of 0.40, only point K lies in the single-phase region. The transition point J is determined by extending a line parallel to GDE from K to the 2-atmosphere pressure curve. A smooth curve now can be drawn to connect the other points, H and I, with J.

3286

The families of curves of X against pressure are handled in the same manner as R. The values of X in the single-phase region are all zero. For the same equivalence ratio and pressure, the transition point occurs at the same effective inlet-air enthalpy as it did for the gas constant R. The remaining points are connected to the transition point by a smooth curve. At 2-atmospheres pressure, an equivalence ratio of 0.30 is represented by the curve A'B'C', and an equivalence ratio of 0.40 by the curve H'I'J'K'.

Values of the ratio of specific heats γ do not vary greatly with effective enthalpy. It has been found adequate to construct smooth curves on the interpolation chart. However, the γ curves should undergo a change in shape at the transition point. Examples of two equivalence ratios at 2-atmospheres pressure are presented. The broad black bands appearing on two of the pressure-γ families of curves represent an area in which the equivalence-ratio lines are grouped too close together to bear reading or labeling. Values in this region are selected from the midpoint of the band.

The preceding methods may also be used to determine the temperature and the thermal properties at any station in the exhaust nozzle. The static pressure must be known at the particular station involved.

REFERENCES

1. Breitwieser, Roland, Gordon, Sanford, and Gammon, Benson: Summary Report on Analytical Evaluation of Air and Fuel Specific-Impulse Characteristics of Several Nonhydrocarbon Jet-Engine Fuels. NACA RM E52L08, 1953.

2. Henneberry, Hugh M.: Effect of Fuel Density and Heating Value on Ram-Jet Airplane Range. NACA RM E51L21, 1952.

3. Gammon, Benson E., Genco, Russell S., and Gerstein, Melvin: A Preliminary Experimental and Analytical Evaluation of Diborane as a Ram-Jet Fuel. NACA RM E50J04, 1950.

4. Price, F. P.: Burning and Detonation of Mixtures of Boron Hydrides with Air and Oxygen. Rep. No. R50A0504, Apparatus Dept., General Electric Co., Mar. 1950. (Proj. HERMES (TU1-2000A), U. S. Army Ord. Dept.)

5. Cook, Preston N., Jr., Lord, Albert M., and Kaye, Samuel: Blow-Out Velocities of Various Petroleum, Slurry, and Hydride Fuels in a $1\frac{7}{8}$-Inch Diameter Combustor. NACA RM E54A28, 1954.

6. Disher, John H., and Rabinowitz, Leonard: Free-Flight Performance of 16-Inch-Diameter Supersonic Ram-Jet Units. III - Four Units Designed for Combustion-Chamber-Inlet Mach Number of 0.245 at Free-Stream Mach Number of 1.8 (Units D-1, D-2, D-3, and D-4). NACA RM E50D07, 1950.

7. North, Warren J.: Summary of Free-Flight Performance of a Series of Ram-Jet Engines at Mach Numbers from 0.80 to 2.20. NACA RM E53K17, 1954.

8. Branstetter, J. Robert, Gibbs, James B., and Kaufman, Warner B.: Magnesium-Slurry Combustion Performance in 6.5-Inch-Diameter Ram-Je Engine Mounted in Connected-Pipe Facility. NACA RM E53E27, 1953.

9. Keenan, Joseph H., and Kaye, Joseph: Gas Tables. John Wiley & Sons, Inc., 1948.

10. Dettwyler, H. Rudolph, and Faget, Maxime A.: Engineering Method of Ram-Jet Thrust Determination Based on Experimentally Obtained Combustor Parameters. NACA RM L53E21, 1953.

11. Tower, Leonard K., and Gammon, Benson E.: Analytical Evaluation of Effect of Equivalence Ratio, Inlet-Air Temperature, and Combustion Pressure on Performance of Several Possible Ram-Jet Fuels. NACA RM E53G14, 1953.

12. Bahr, Donald W.: Evaporation and Spreading of Isooctane Sprays in High-Velocity Air Streams. NACA RM E53I14, 1953.

3286

TABLE I. - SUMMARY OF COMBUSTION PERFORMANCE WITH FINAL COMBUSTOR CONFIGURATION

Run	Time from start of combustion, sec	W_a, lb/sec	$p_{2,b}$, lb/sq in. abs	P_4, lb/sq in. abs	$T_{2,b}$, °F	Equivalence ratio	W_f, lb/sec	$V_{2,b}$, ft/sec	$M_{2,b}$	η	S_a^*, sec	$\frac{1}{S_f^*}$, 1/sec	$\frac{P_2-P_3}{q_{2,b}}$	$\frac{\rho_{2,b}}{\rho_3}$	C_f	T_3/T_1	M_3	Combustor wall temperature, °F
8	1.2	16.26	29.80	18.91	217	0.491	0.610	265	0.209	87.34	145.6	0.258×10^{-3}	4.094	7.26	1.069	4.98	0.761	220
	3.2	15.87	29.87	19.96	221	.498	.606	257	.202	98.05	148.8	.255	3.774	7.18	1.079	5.16	.722	320
	5.7	11.18	25.14	18.23	226	.715	.610	219	.171	89.07	163.3	.334	4.159	7.60	1.052	5.95	.616	480
	7.8	8.65	22.21	17.47	232	.927	.612	203	.158	84.65	175.0	.405	3.504	7.83	1.053	6.58	.538	600
	10.1	15.67	29.90	19.38	244	.506	.604	262	.202	99.80	150.2	.257	3.361	7.08	1.070	5.19	.733	725
9	1.9	16.22	28.44	18.86	182	.395	.489	261	.211	85.34	136.4	.221	3.904	6.856	1.061	4.74	.714	245
	3.6	14.43	26.76	18.24	183	.434	.478	245	.202	90.82	142.0	.233	4.140	7.002	1.061	5.04	.685	285
12	2.0	6.09	11.75	5.07	56	.523	.243	192	.173	90.63	145.0	.275	13.26	14.47	.986	6.62	.987	55
	6.2	6.13	12.04	5.73	58	.511	.239	190	.171	93.74	145.6	.268	12.83	13.19	.977	6.64	.903	100
	10.6	6.19	12.10	5.85	60	.503	.238	191	.172	93.04	144.6	.266	10.80	11.80	.975	6.39	.914	170
	14.8	6.23	12.15	6.20	65	.472	.224	193	.173	97.03	143.7	.250	10.45	11.05	.974	6.26	.866	280
	19.5	6.29	11.97	6.10	70	.417	.200	198	.176	86.33	137.3	.232	10.64	10.39	.956	5.76	.851	345
	24.3	5.21	10.40	5.47	74	.485	.193	193	.171	97.53	144.4	.256	10.76	10.76	.964	6.23	.830	400
	27.2	5.26	10.26	5.28	75	.468	.188	197	.174	90.81	141.7	.252	10.58	10.59	.963	6.00	.849	430
	29.7	5.27	10.23	5.32	77	.455	.183	198	.175	95.16	141.2	.246	11.22	10.50	.970	5.98	.819	450
13	5.6	2.15	4.07	2.56	46	.107	.0176	190	.173	98.13	90.78	.090	2.98	2.73	.640	2.54	.166	45
	9.9	2.13	4.38	2.55	46	.139	.0226	177	.161	102.2	99.58	.106	3.76	3.28	.641	2.99	.195	45
	14.9	2.11	4.18	2.55	46	.132	.0213	181	.165	96.21	95.97	.105	3.00	3.06	.644	2.82	.215	50
	23.0	2.09	4.18	2.50	46	.139	.0221	180	.164	90.65	95.89	.110	3.06	3.04	.638	2.81	.198	65
	26.3	1.74	3.71	2.38	47	.151	.0201	172	.156	98.01	100.9	.114	2.59	3.44	.638	3.17	.265	70
	28.7	1.62	3.55	2.32	47	.161	.0199	167	.152	99.38	103.5	.119	3.01	3.63	.640	3.33	.258	70
14	26.1	2.11	5.52	2.65	50	.364	.0587	143	.129	88.74	132.2	.210	6.32	6.39	.669	5.60	.293	50
	32.0	2.11	5.67	2.65	51	.388	.0625	142	.128	88.92	135.0	.219	6.89	6.66	.665	5.80	.310	50
	38.1	2.10	5.65	2.72	53	.406	.0651	142	.128	88.67	137.1	.226	8.01	6.70	.675	5.86	.260	55
	47.7	2.10	5.05	2.64	55	.279	.0447	153	.138	87.46	120.4	.177	4.77	5.36	.662	4.66	.337	62
	55.9	2.10	4.88	2.61	56	.236	.0378	162	.146	90.68	114.6	.157	3.92	4.89	.652	4.30	.341	75
	59.9	2.10	4.85	2.61	57	.232	.0372	164	.147	92.24	114.5	.155	3.38	4.89	.656	4.28	.371	80
	66.4	1.60	4.05	2.41	58	.296	.0361	150	.135	90.88	124.0	.182	4.38	5.75	.650	4.96	.385	100
	73.9	1.68	4.13	2.40	60	.269	.0344	154	.138	91.45	120.5	.170	4.31	5.42	.650	4.67	.386	80

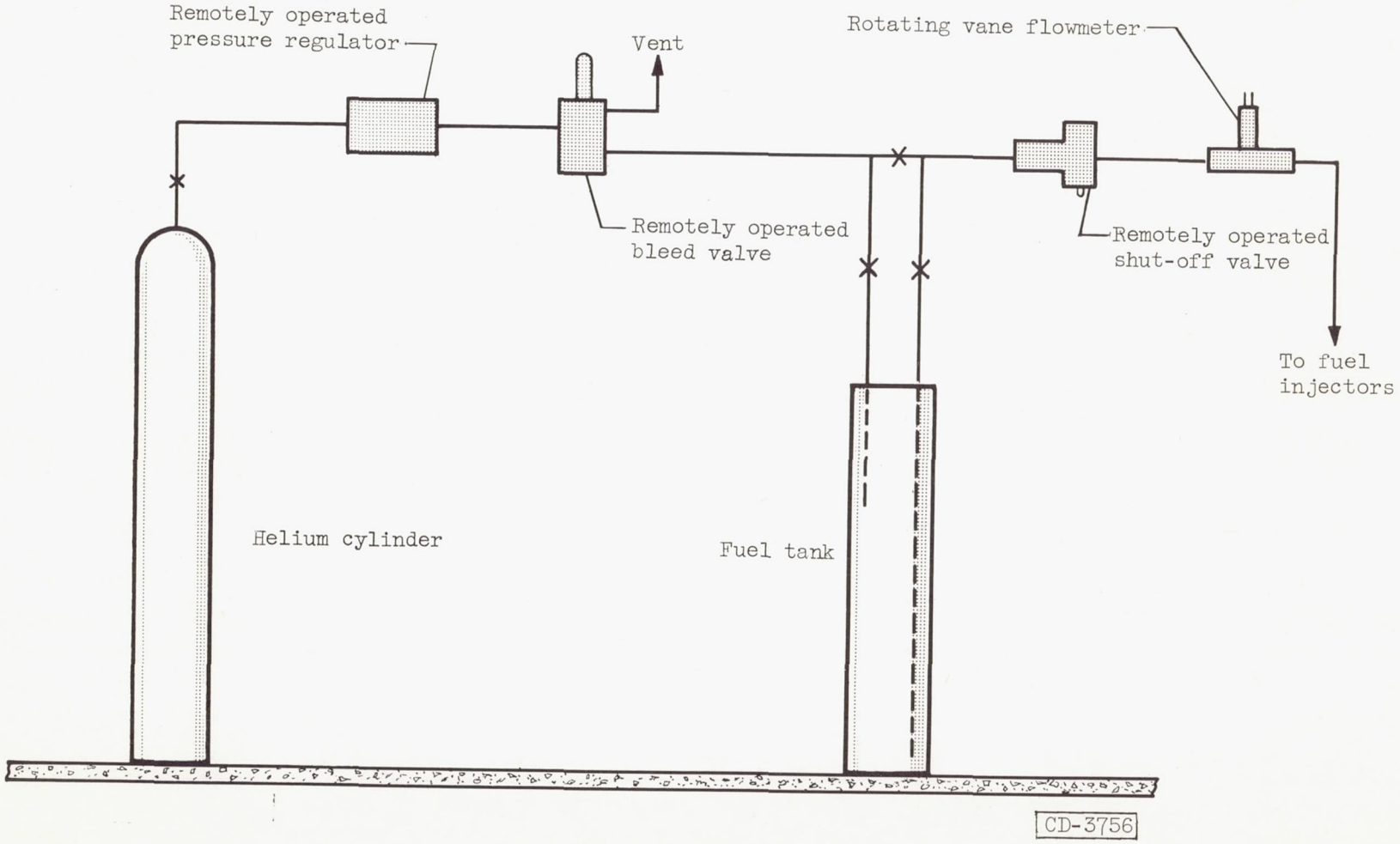


Figure 1. -Fuel system.

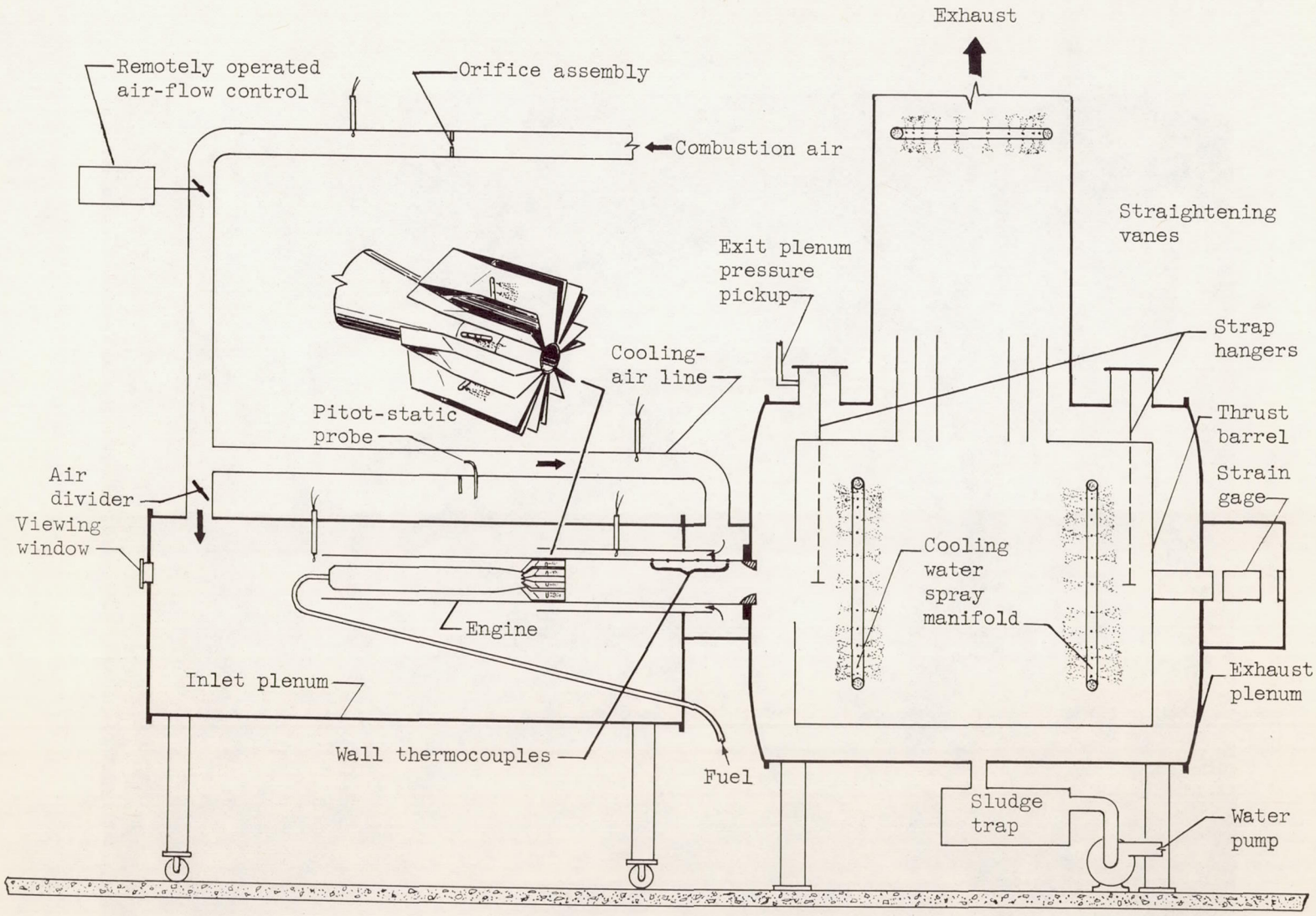
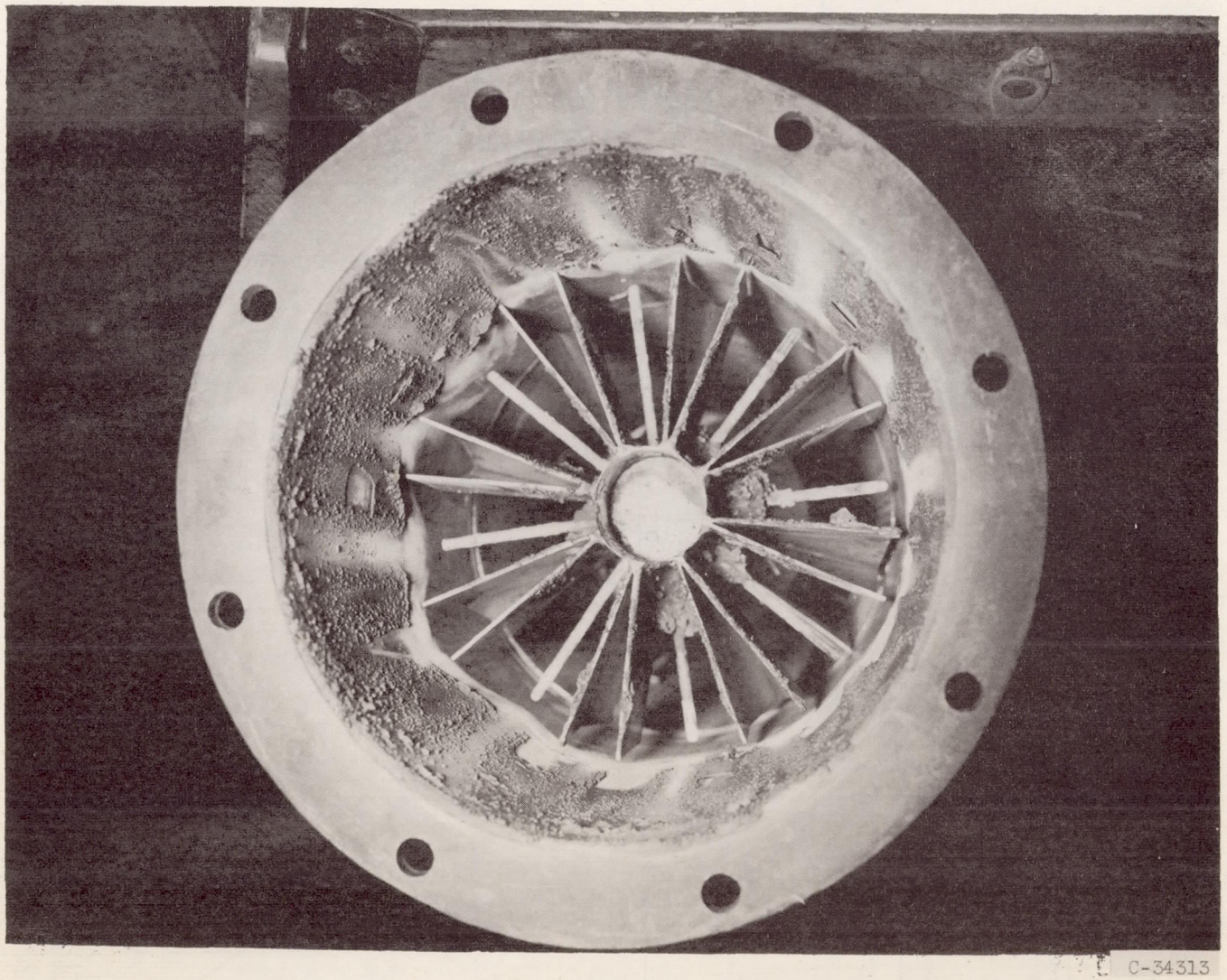


Figure 2. - Ramjet installation.

CD-3755

(a) View from side.

Figure 3. - Installation of fuel injector and flame holder.



(b) View from downstream end.

Figure 3. - Concluded. Installation of fuel injector and flame holder.

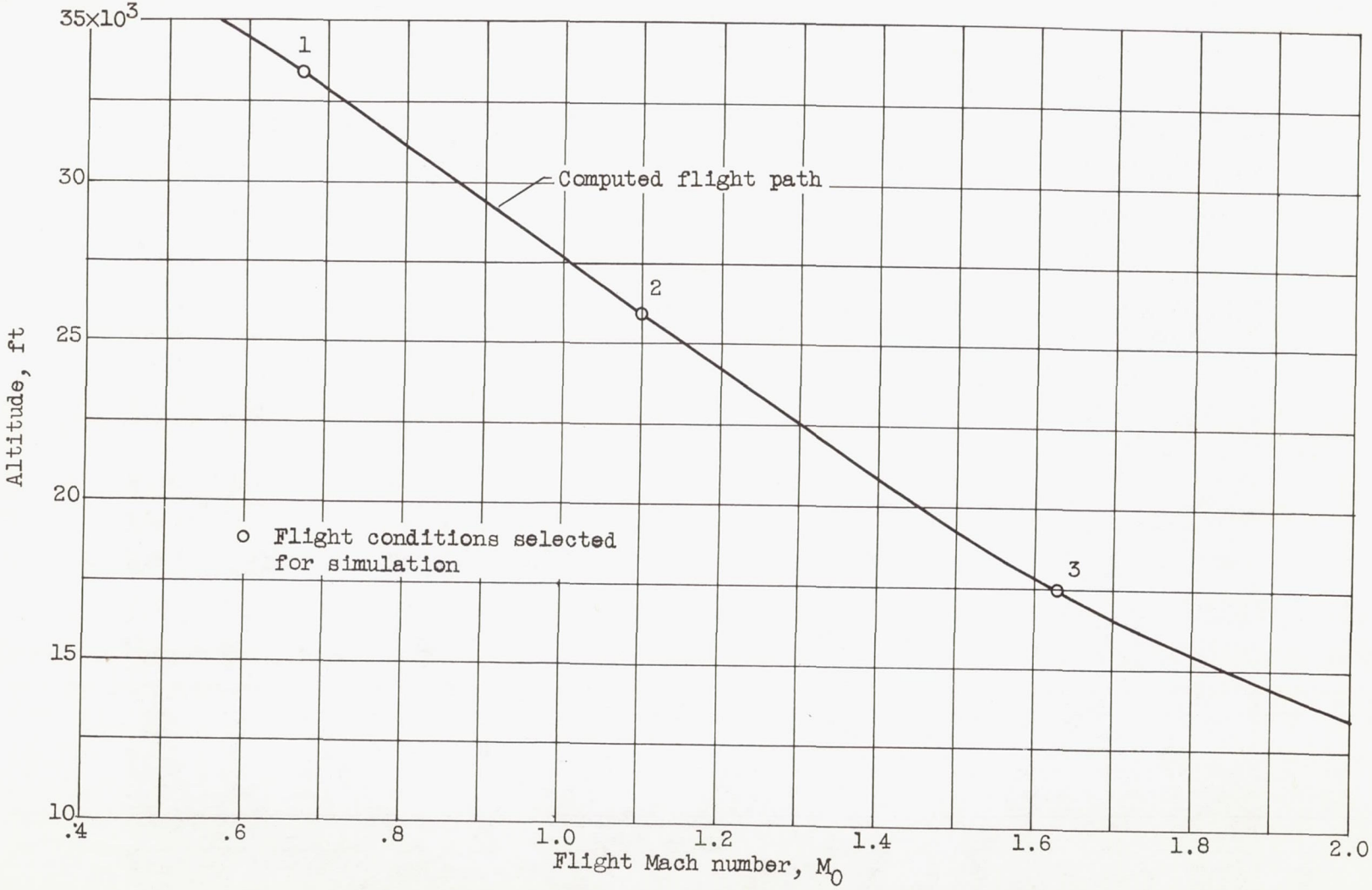


Figure 4. - Anticipated flight path.

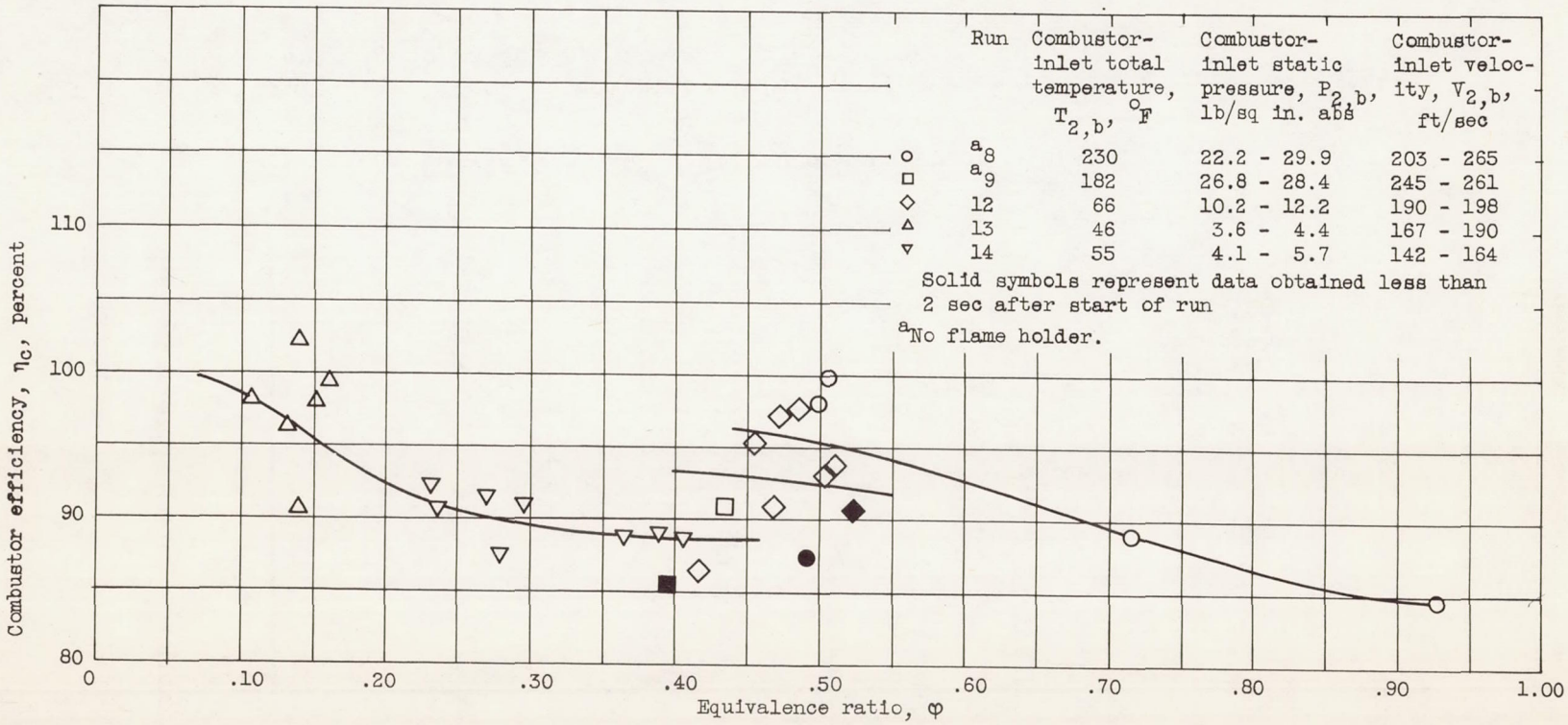


Figure 5. - Effect of equivalence ratio on combustor efficiency.

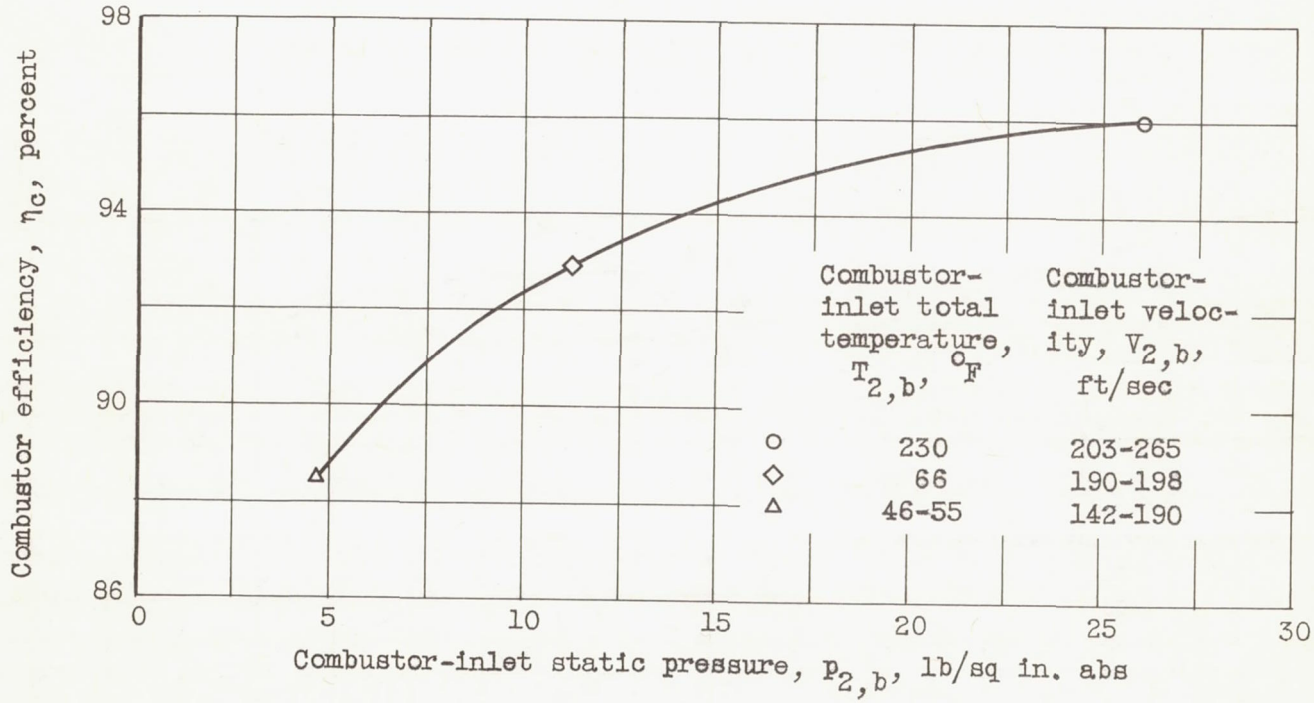


Figure 6. - Effect of combustor-inlet static pressure on combustor efficiency. Equivalence ratio, 0.45.

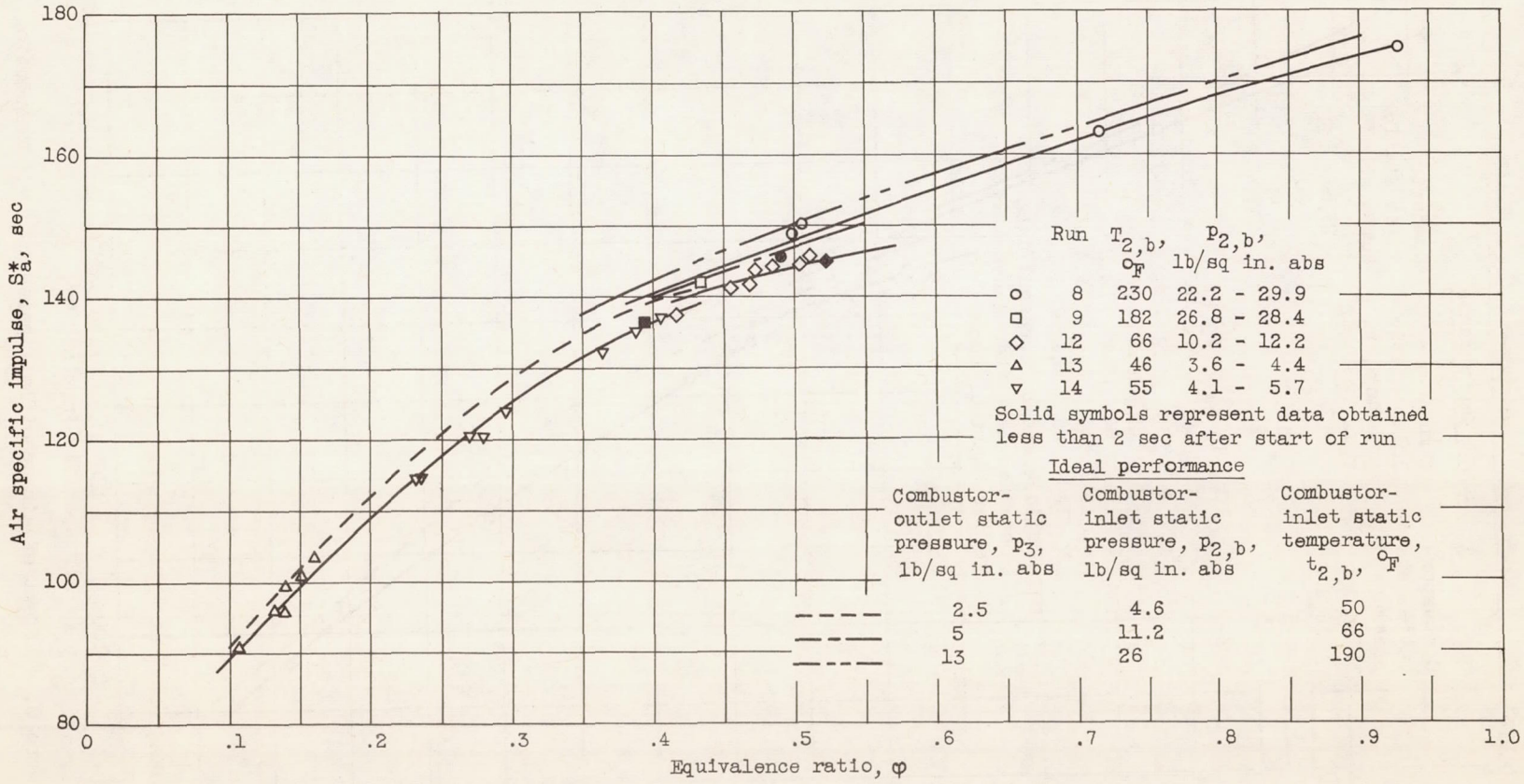


Figure 7. - Effect of equivalence ratio on air specific impulse.

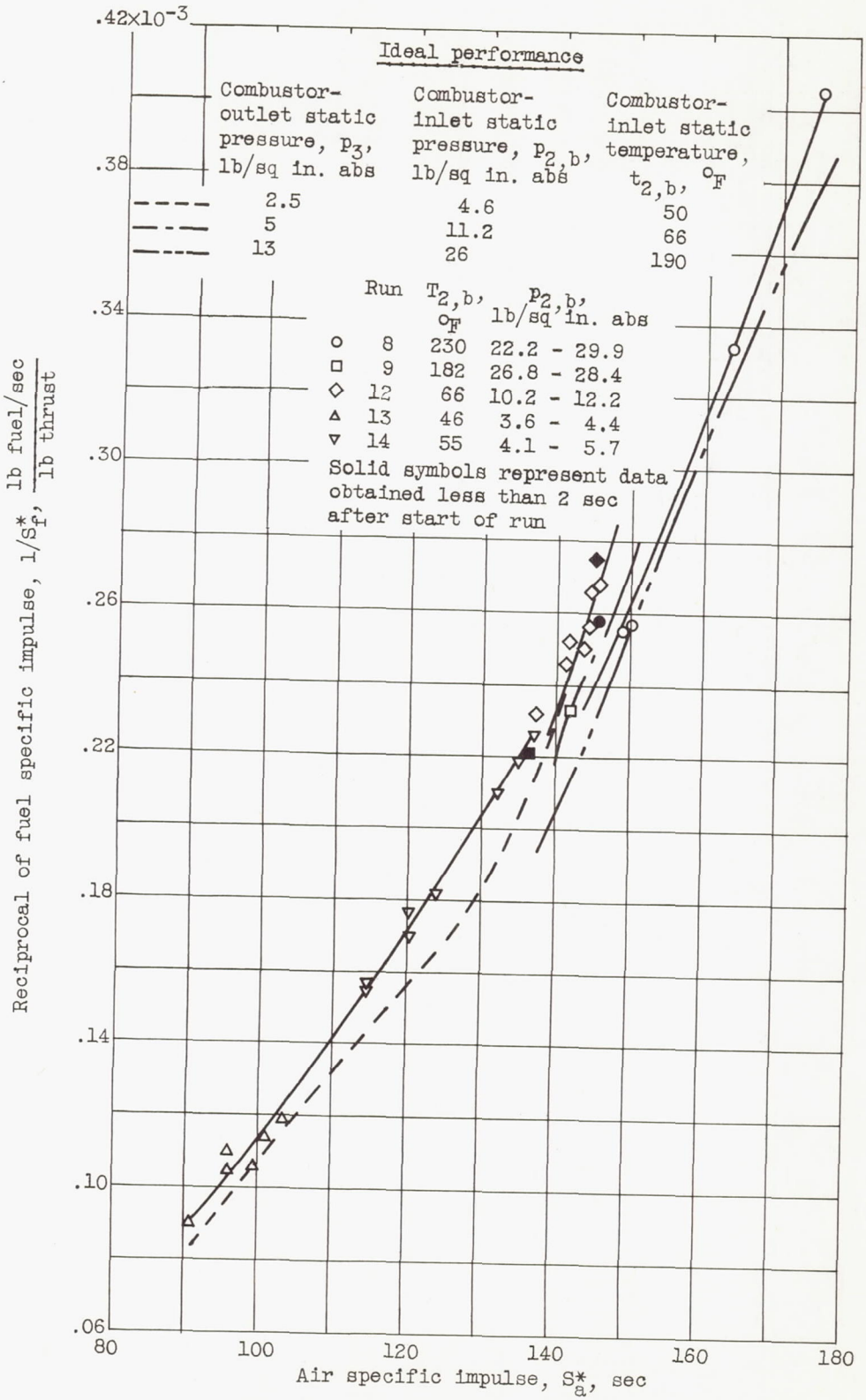


Figure 8. - Effect of air specific impulse on fuel consumption.

3286

3286

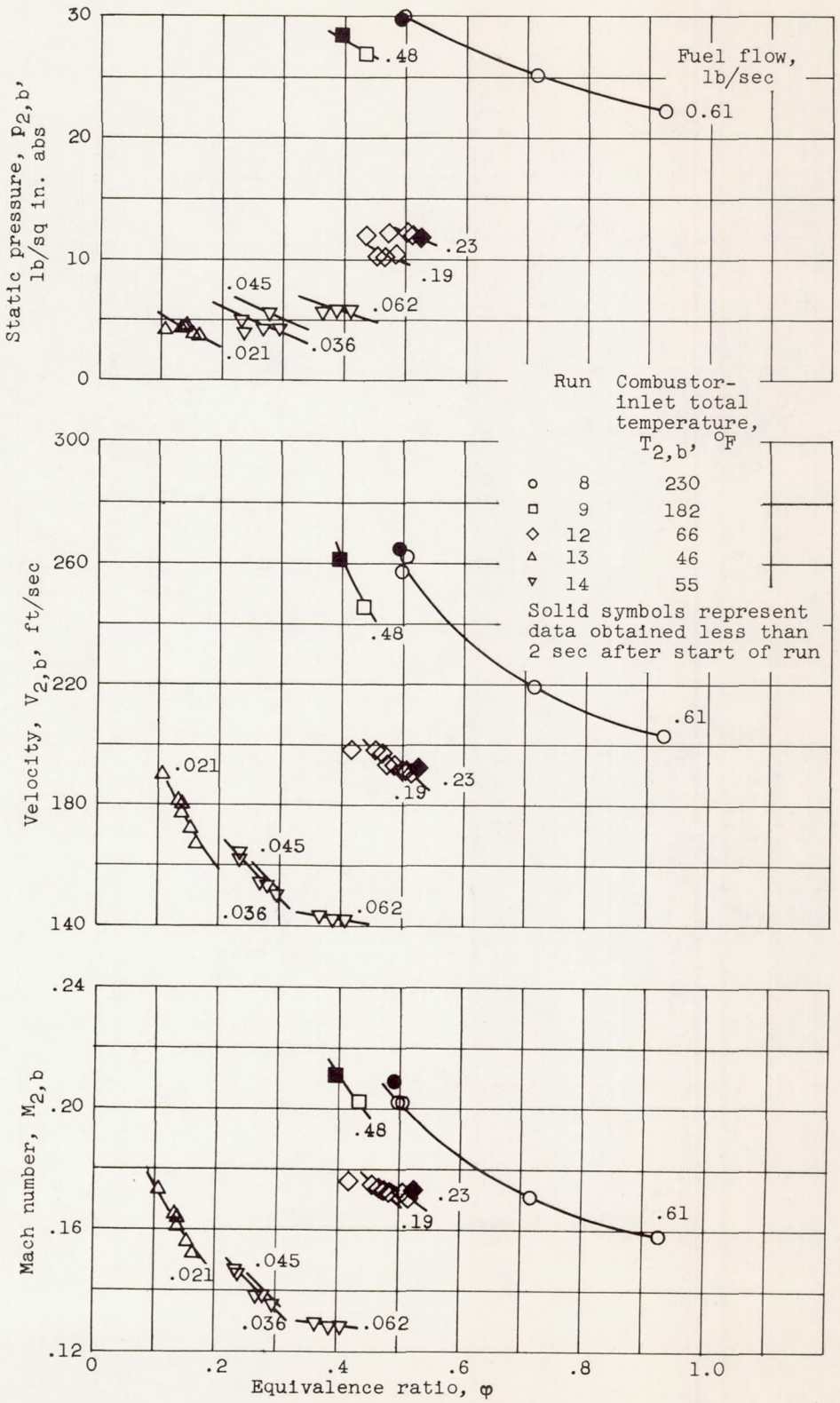


Figure 9. - Combustor-inlet conditions.

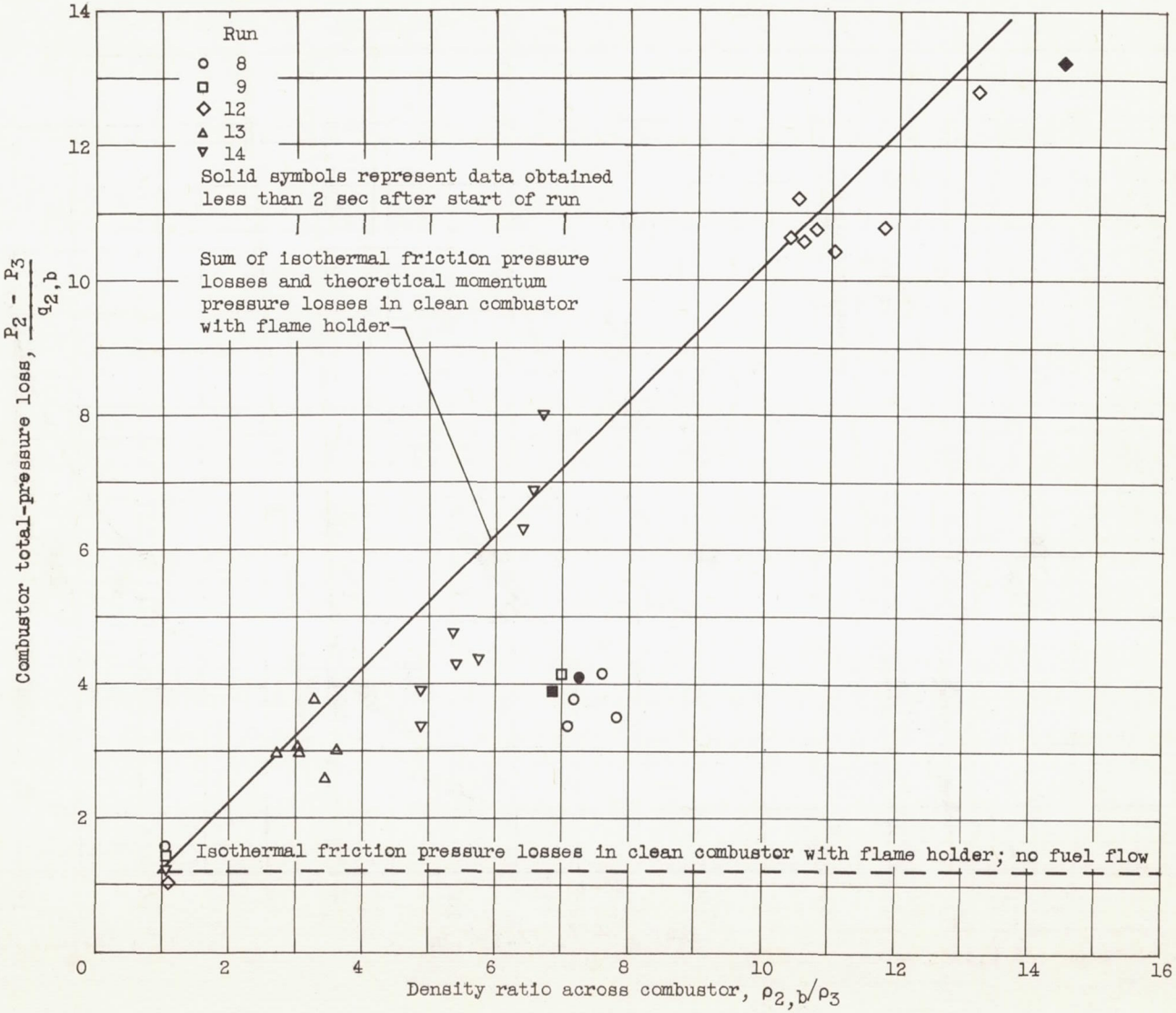


Figure 10. - Combustor pressure losses.

3286

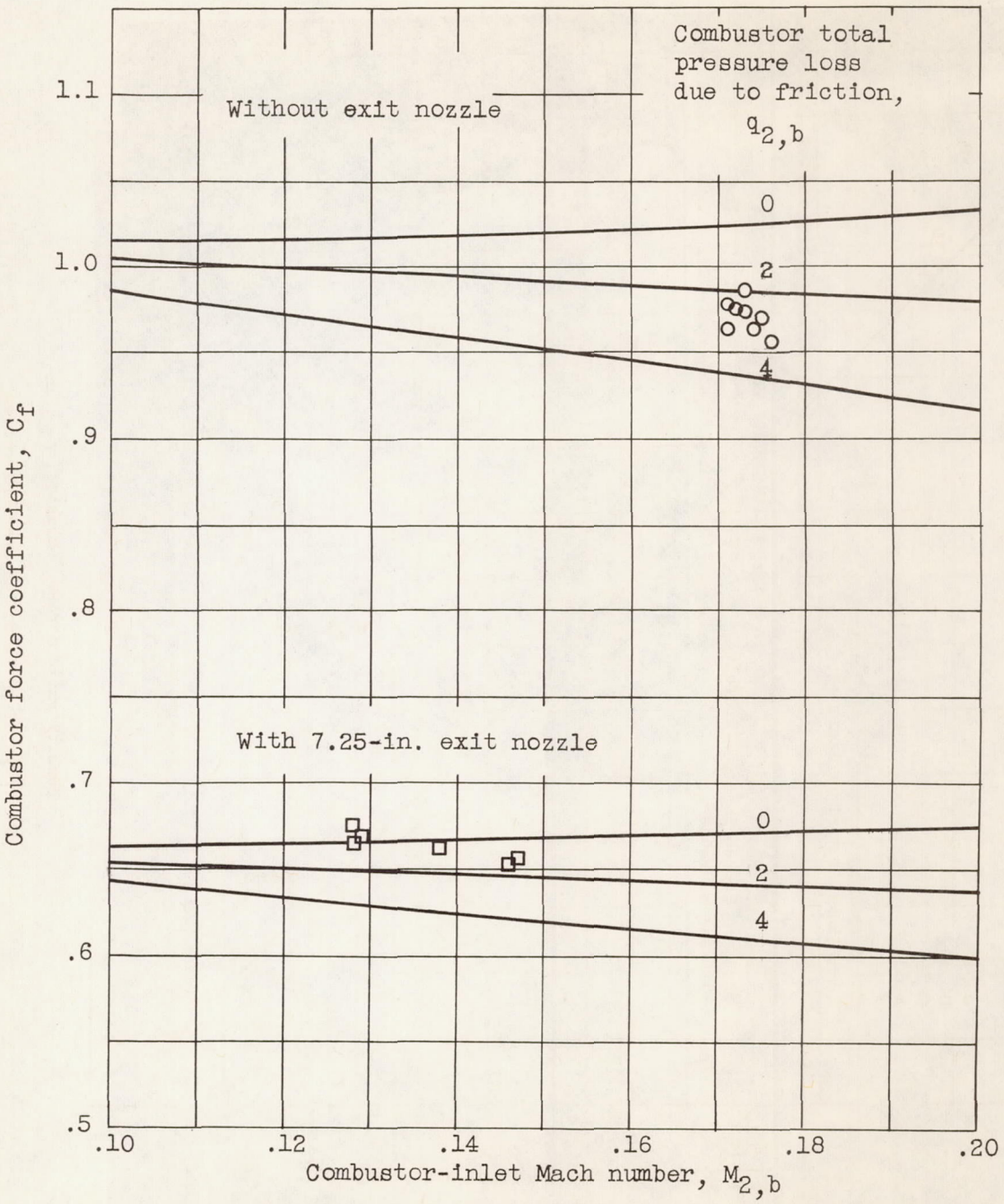
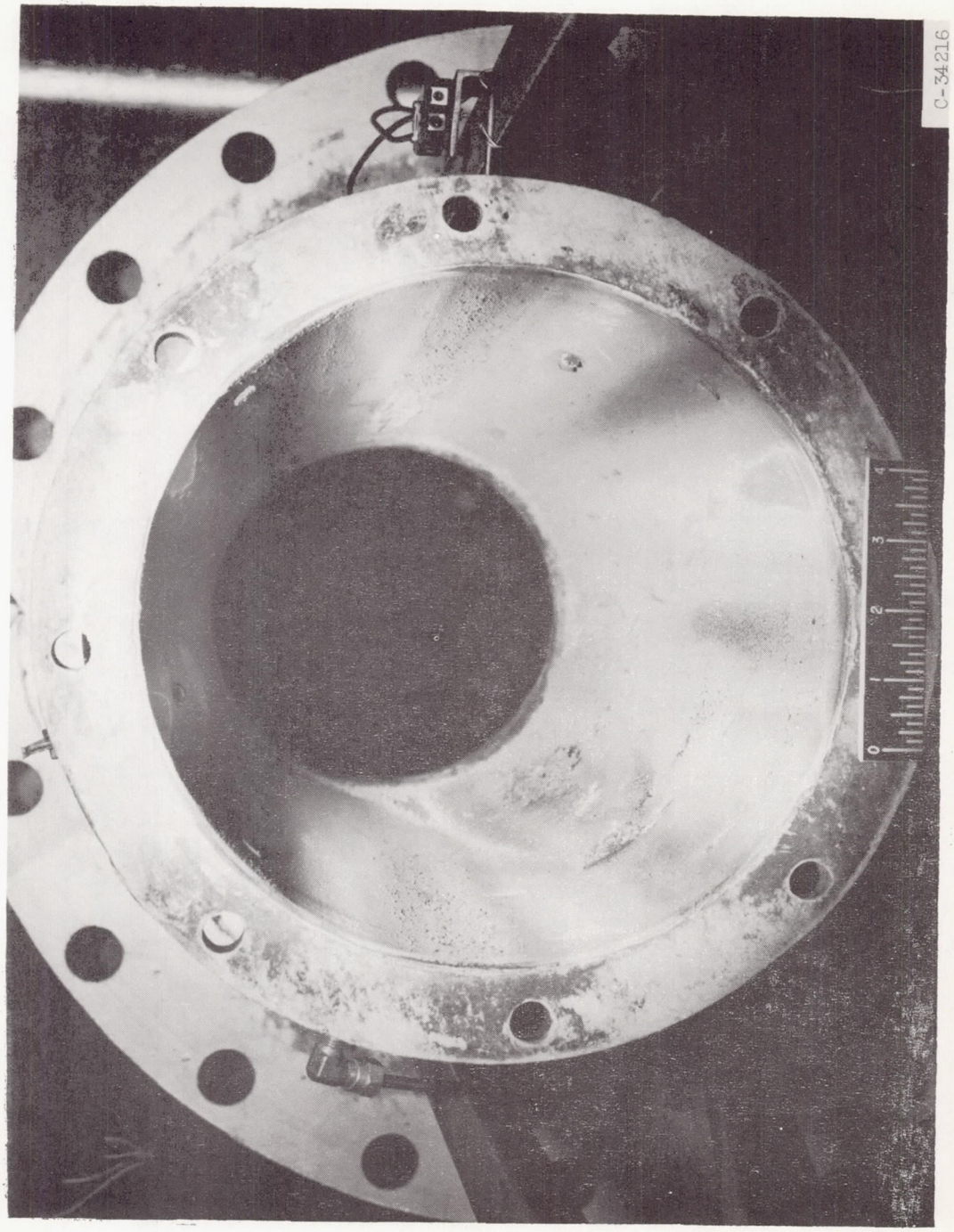
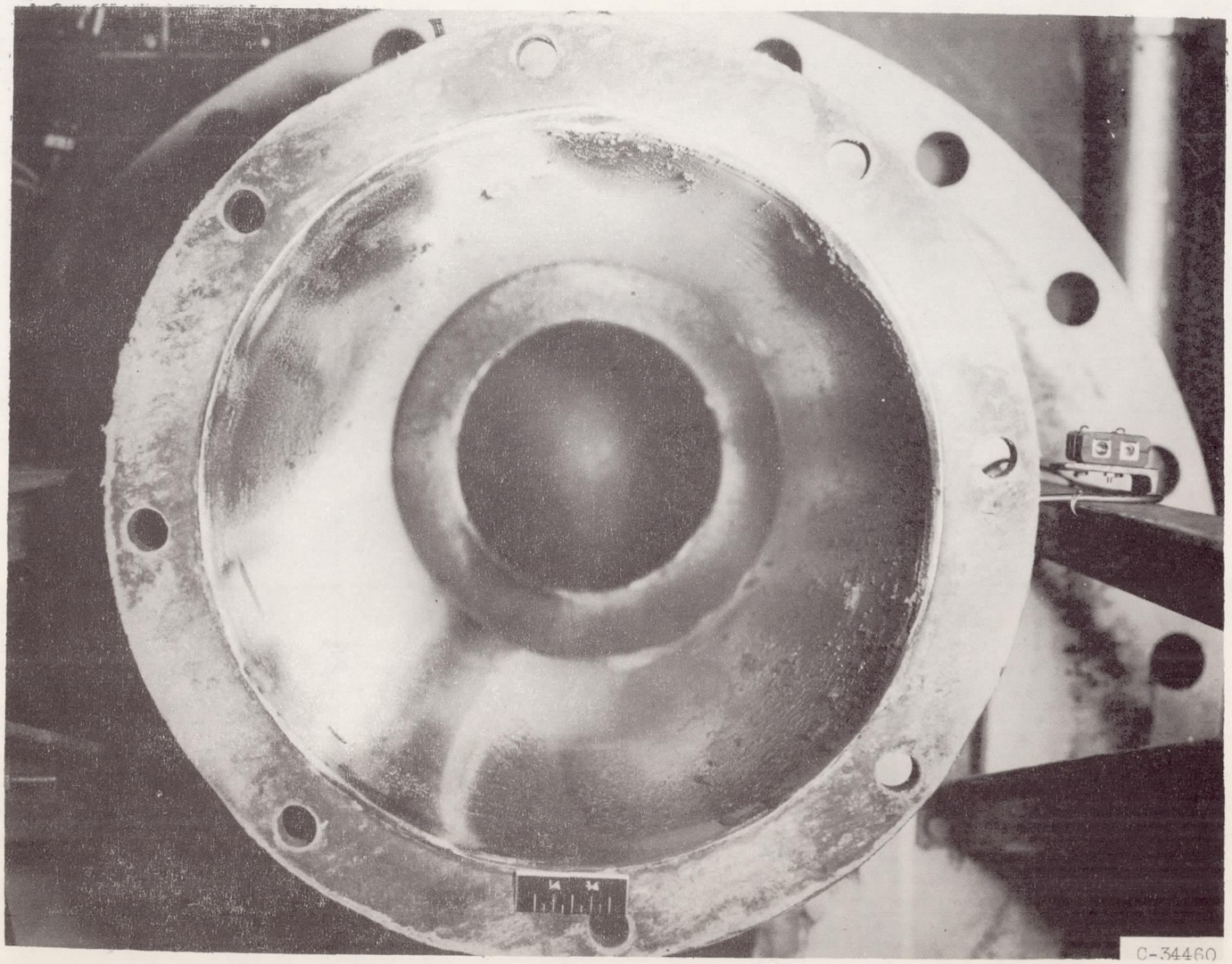


Figure 11. - Effect of combustor-inlet conditions on combustor force coefficient.



(a) Simulated low altitude.

Figure 12. - Deposits on combustor wall.



(b) Simulated high altitude.

Figure 12. - Concluded. Deposits on combustor wall.

3286

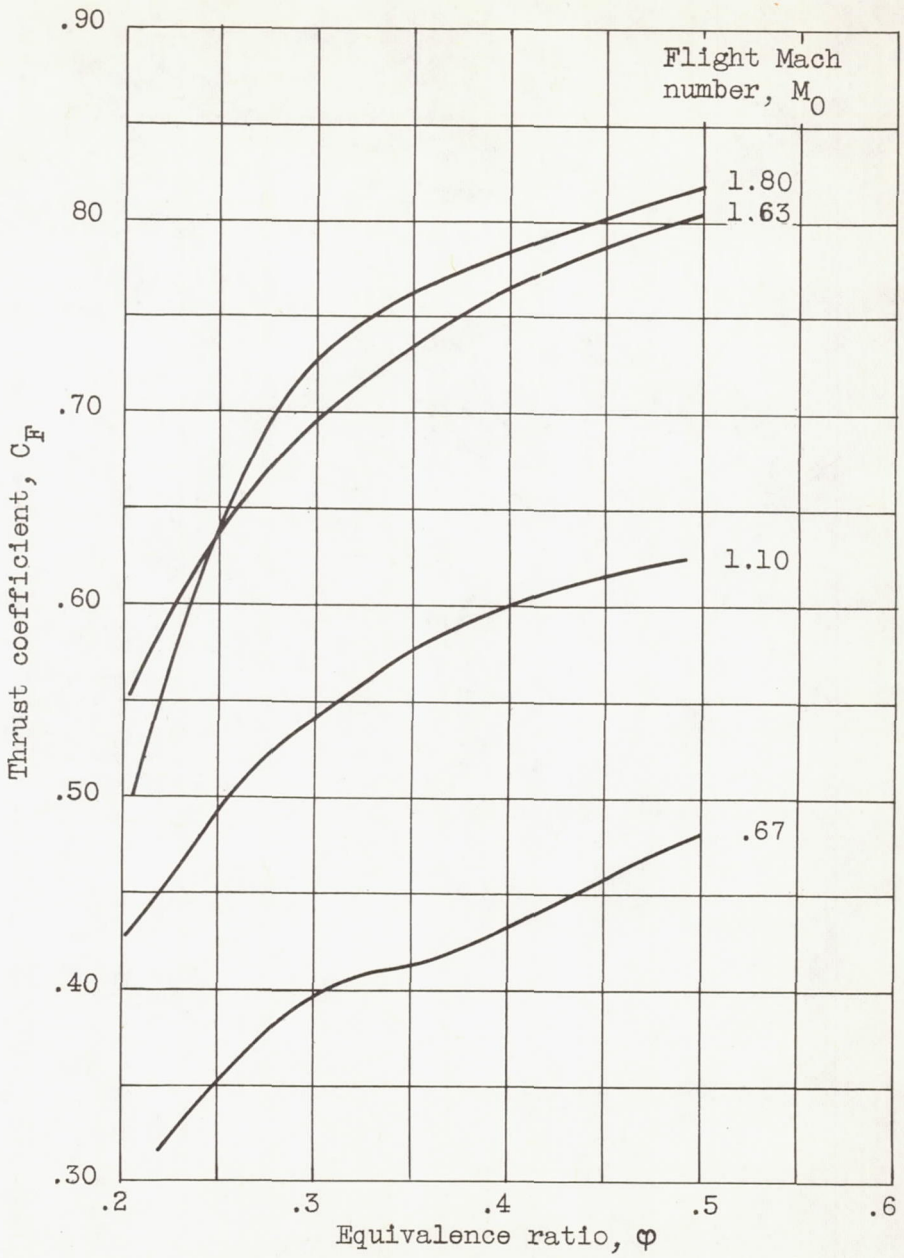


Figure 13. - Variation of thrust coefficient with equivalence ratio for several flight Mach numbers along proposed flight path.

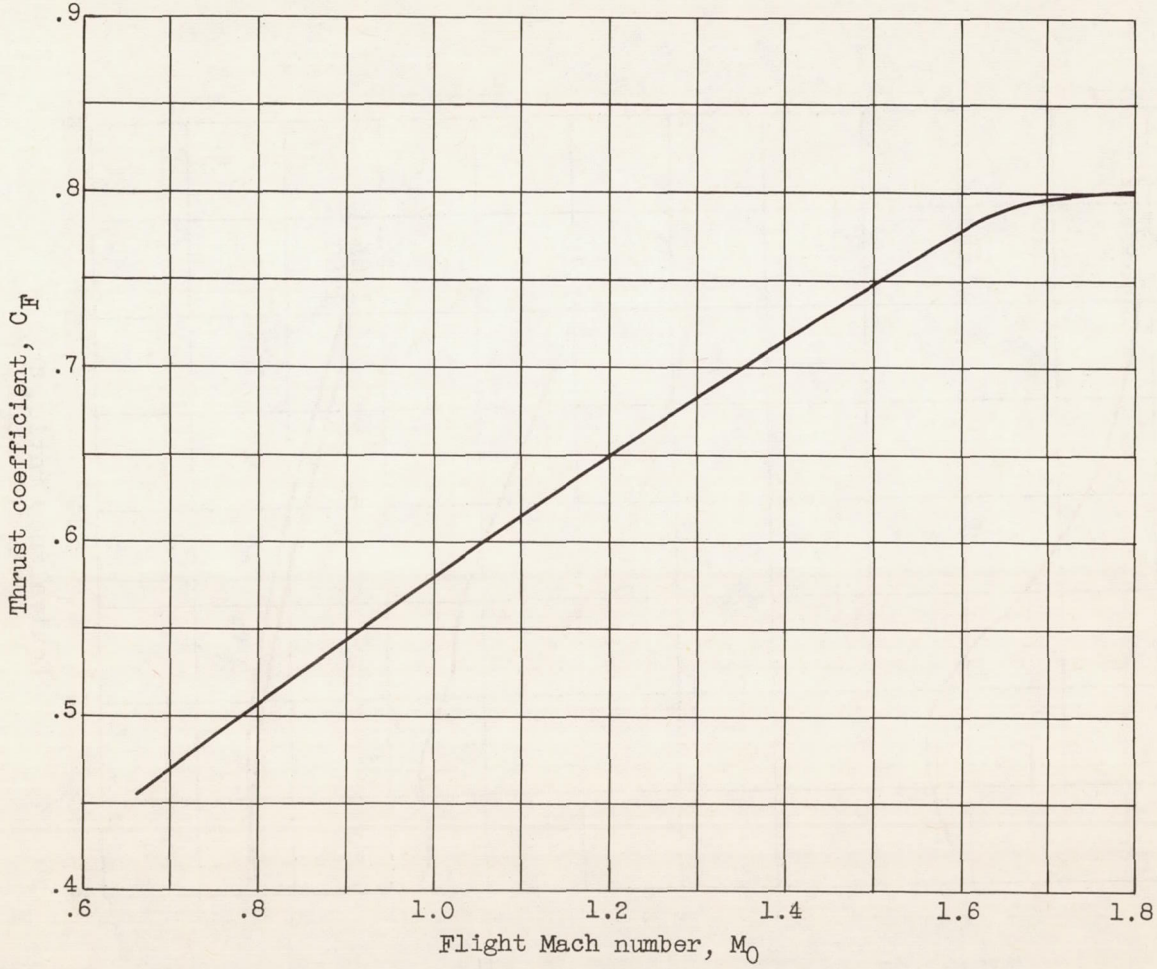


Figure 14. - Variation of thrust coefficient with flight Mach number for proposed flight path at equivalence ratio of 0.45.

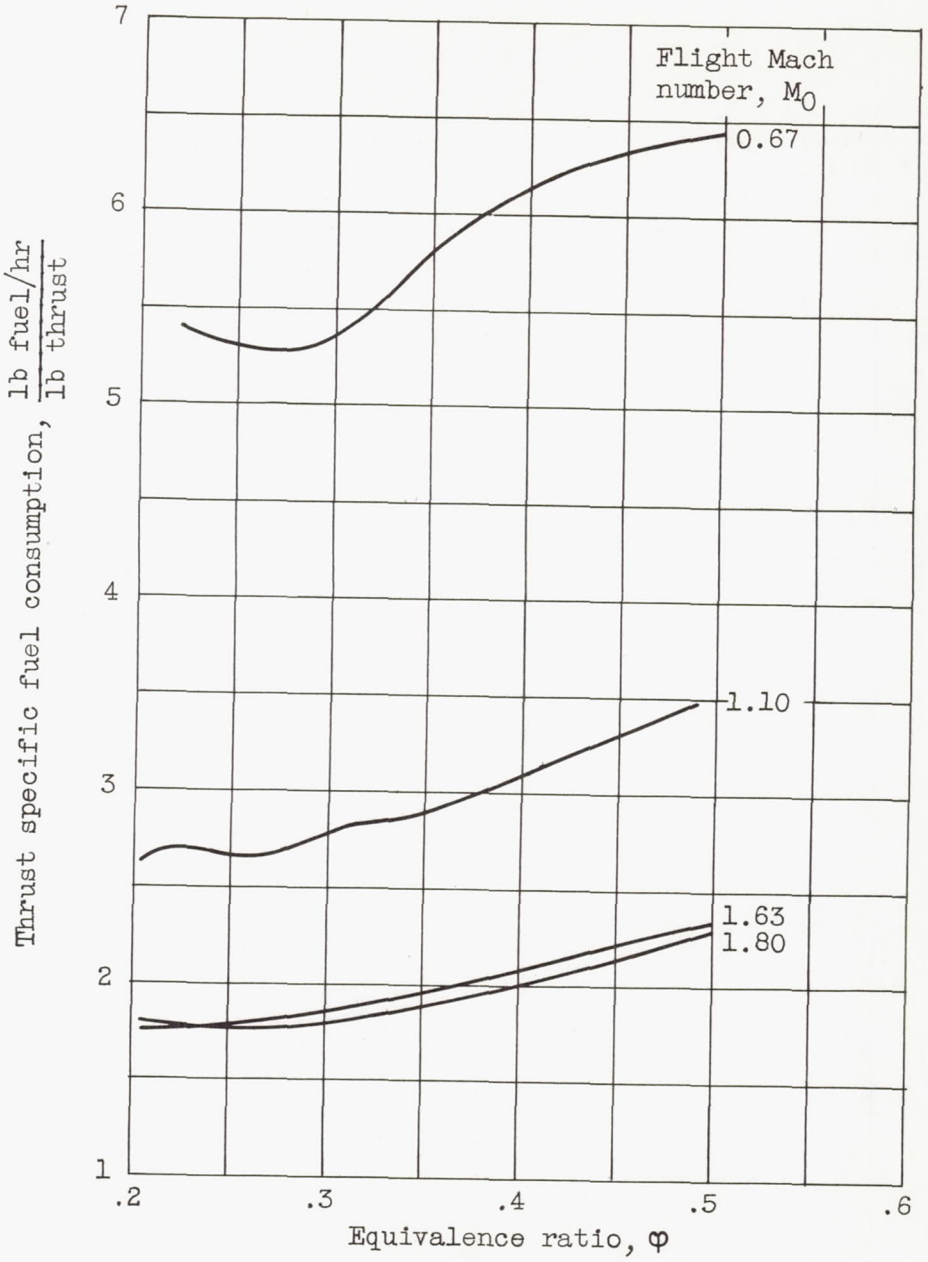


Figure 15. - Variation of thrust specific fuel consumption with equivalence ratio for several flight Mach numbers along proposed flight path.

3286

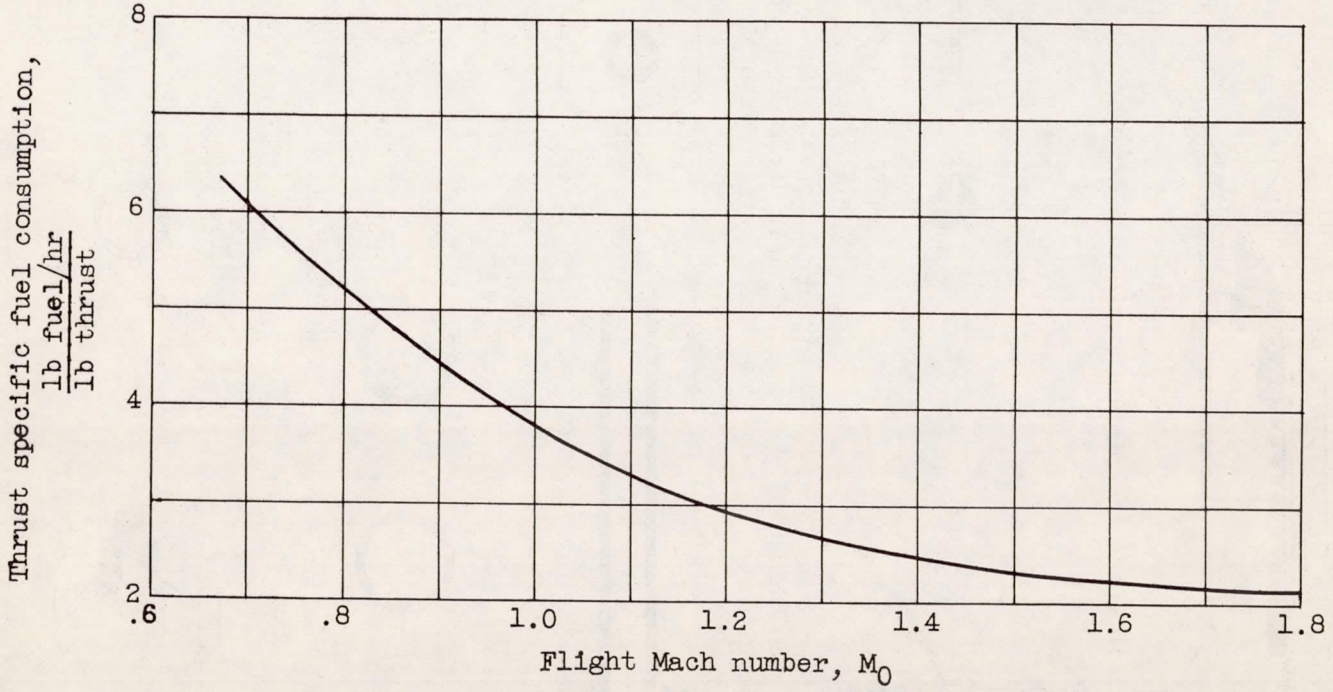
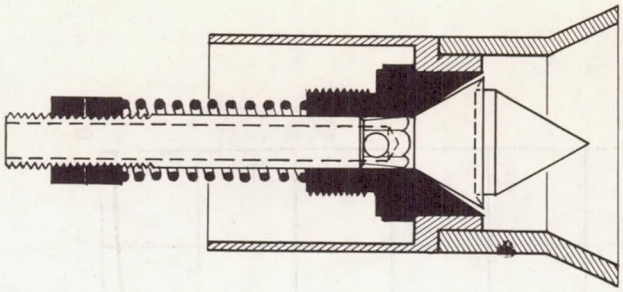
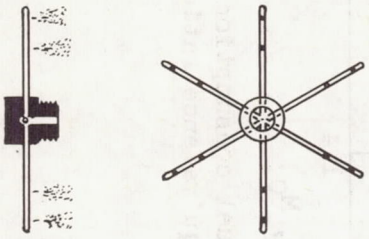


Figure 16. - Variation of thrust specific fuel consumption with flight Mach number for proposed flight path at equivalence ratio of 0.45.

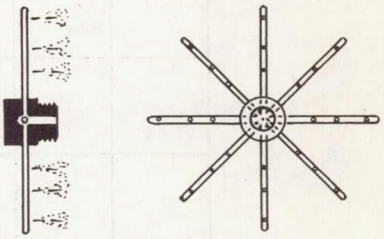
3286



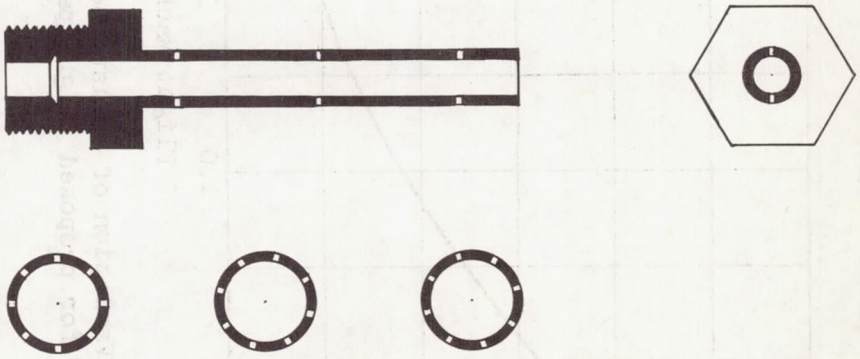
(a) Fuel injector A: pintle nozzle with 50° shroud.



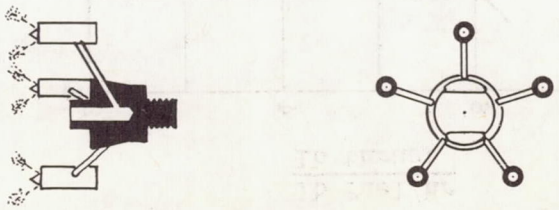
(b) Fuel injector B: 12 orifice; 6 spoke, 0.0550 inch diameter; contrastream injection.



(c) Fuel injector C: 8 spoke; 24 orifice; 0.0550 inch diameter; contrastream injection.



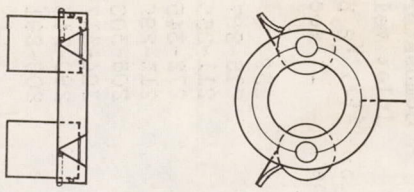
(d) Fuel injector D: 24 orifice tube; 0.0550 inch diameter; radial injection.



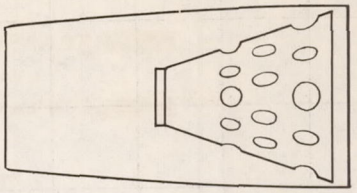
CD-3758

(e) Fuel injector E: 5 point; pintle nozzle; downstream injection.

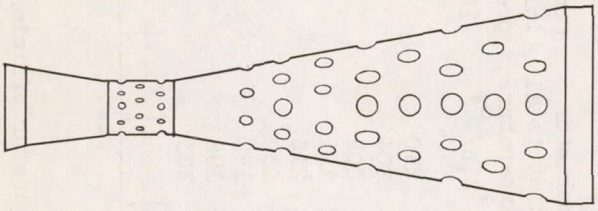
Figure 17. - Fuel injectors.



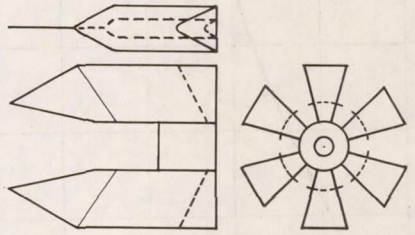
(a) Flame holder A: annular V-gutter; 30-percent blocked area.



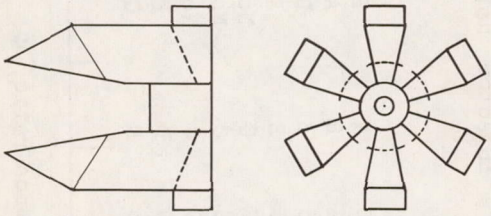
(b) Flame holder B: shrouded can; 65-percent open area.



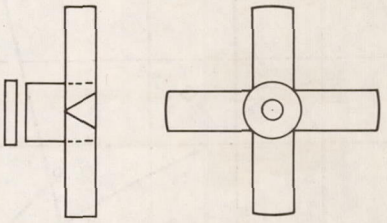
(c) Flame holder C: can type; 133-percent open area.



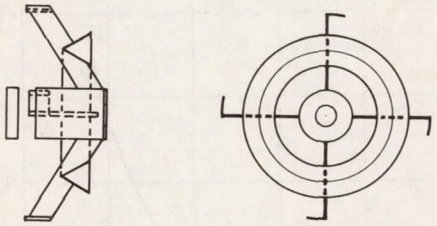
(d) Flame holder D: radial V-gutter; 6 elements; 30-percent blocked area.



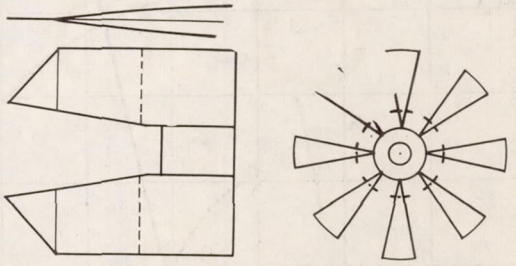
(e) Flame holder E: radial V-gutter; 6 elements, 50-percent blocked area.



(f) Flame holder F: crossed V-gutter; 40-percent blocked area.



(g) Flame holder G: annular V-gutter; 40-percent blocked area.



(h) Flame holder H: radial V-gutter; 8 elements; 30-percent blocked area.

CD-3757

Figure 18. - Flame holders.

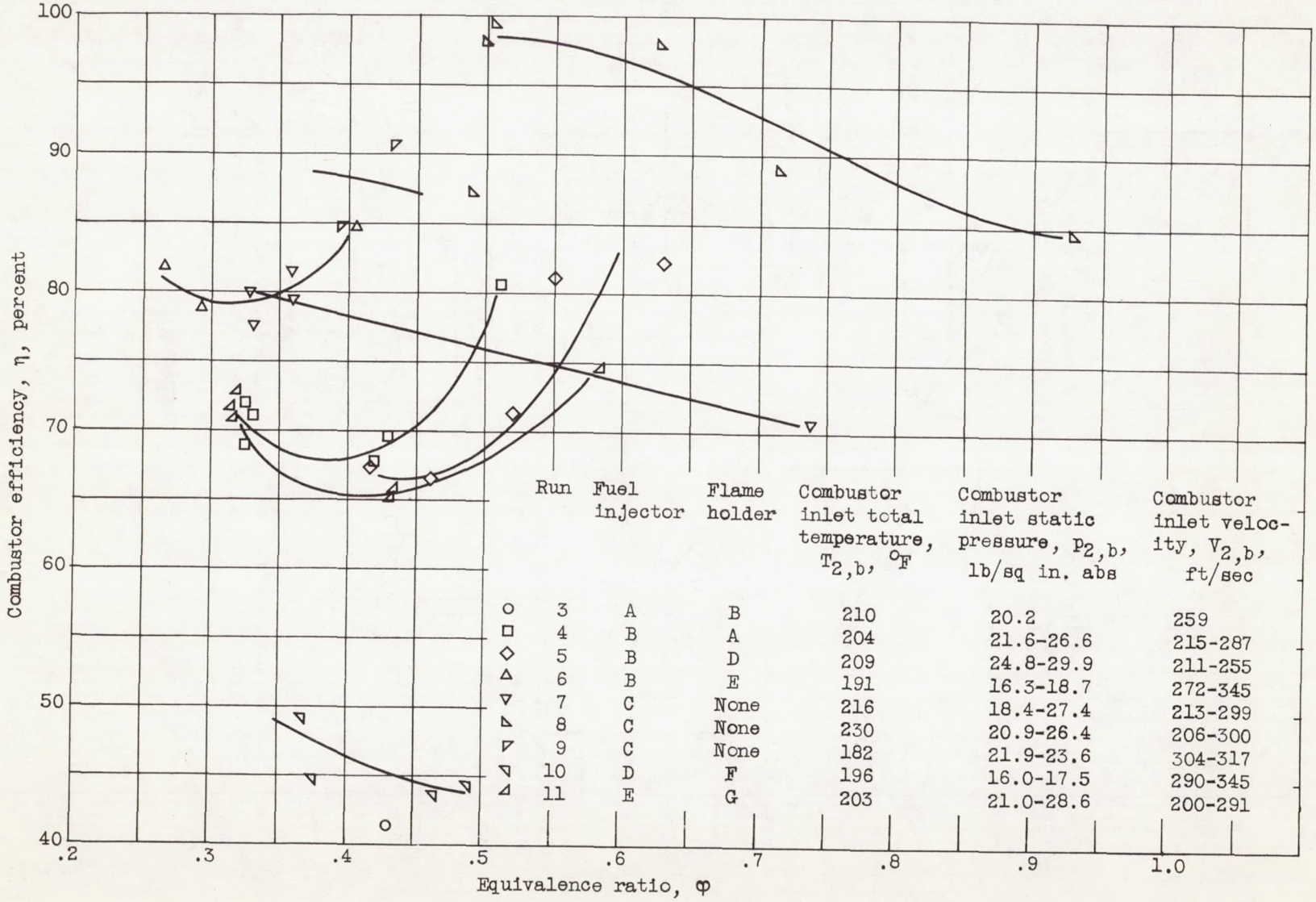


Figure 19. - Effect of combustor configuration on combustor efficiency.

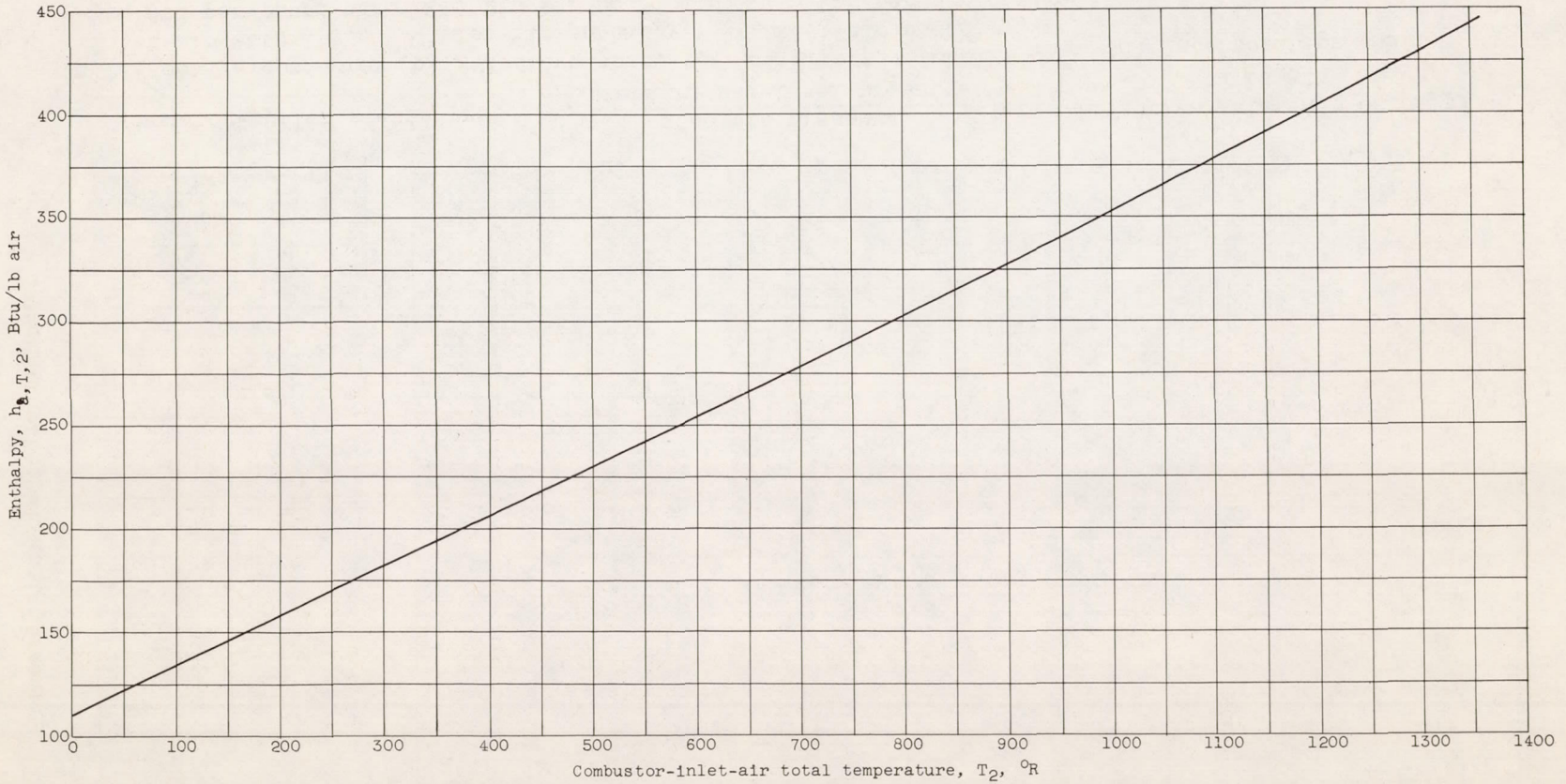
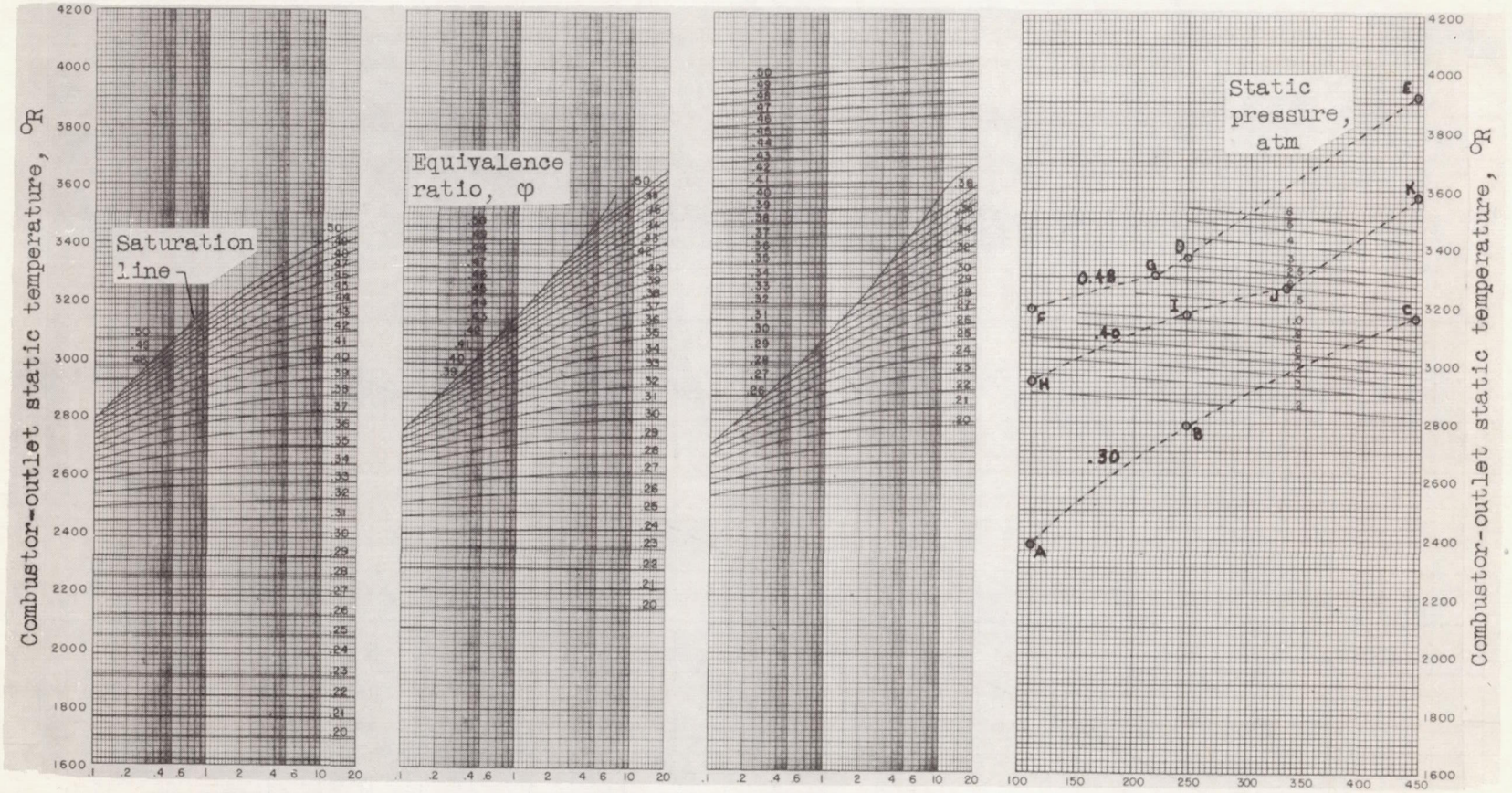


Figure 20. - Total enthalpy of air.



Combustor-outlet static pressure, $\frac{\text{absolute pressure}}{\text{standard sea-level pressure}}$, atm

Effective inlet-air enthalpy, Btu/lb air

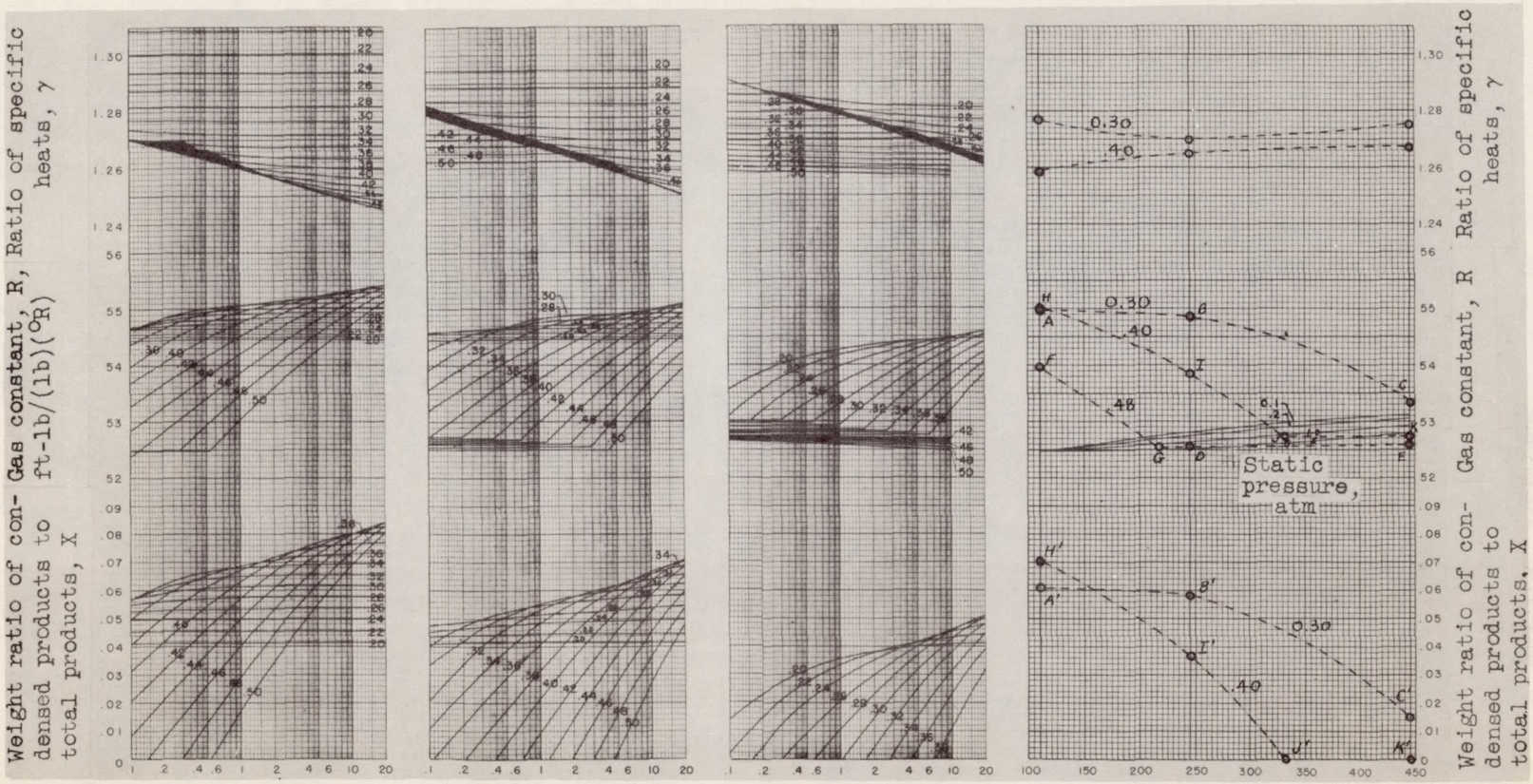
(a) Effective combustor inlet-air enthalpy, 110 Btu per pound air.

(b) Effective combustor inlet-air enthalpy, 245 Btu per pound air.

(c) Effective combustor inlet-air enthalpy, 445 Btu per pound air.

(d) Interpolation chart.

Figure 21. - Combustor-outlet static temperature of pentaborane-air mixtures. (A large working copy of this fig. may be obtained by using the request card bound in the back of the report.)



Combustor-outlet static pressure, $\frac{\text{absolute pressure}}{\text{standard sea-level pressure}}$, atm Effective inlet-air enthalpy, Btu/lb air

(a) Effective combustor inlet-air enthalpy, 110 Btu per pound air.
(b) Effective combustor inlet-air enthalpy, 245 Btu per pound air.
(c) Effective combustor inlet-air enthalpy, 445 Btu per pound air.
(d) Interpolation chart.

Figure 22. - Thermal properties of combustion products of pentaborane-air mixtures. (A large working copy of this fig. may be obtained by using the request card bound in the back of the report.)

NACA - Langley Field, Va.